

# Journal Pre-proof

Synthesis and structure-activity relationship studies of  $\alpha$ -naphthoflavone derivatives as CYP1B1 inhibitors

Jinyun Dong, Zengtao Wang, Jiahua Cui, Qingqing Meng, Shaoshun Li



PII: S0223-5234(19)31090-6

DOI: <https://doi.org/10.1016/j.ejmech.2019.111938>

Reference: EJMECH 111938

To appear in: *European Journal of Medicinal Chemistry*

Received Date: 17 August 2019

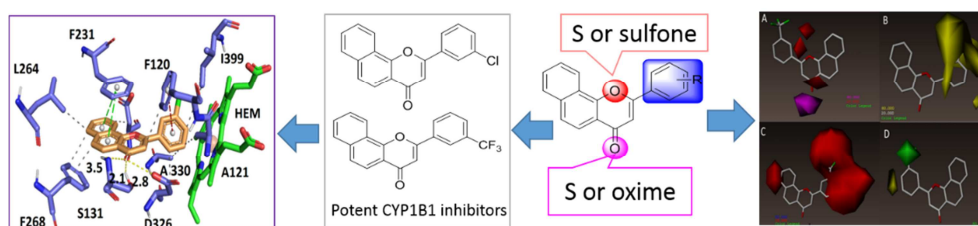
Revised Date: 28 November 2019

Accepted Date: 30 November 2019

Please cite this article as: J. Dong, Z. Wang, J. Cui, Q. Meng, S. Li, Synthesis and structure-activity relationship studies of  $\alpha$ -naphthoflavone derivatives as CYP1B1 inhibitors, *European Journal of Medicinal Chemistry* (2020), doi: <https://doi.org/10.1016/j.ejmech.2019.111938>.

This is a PDF file of an article that has undergone enhancements after acceptance, such as the addition of a cover page and metadata, and formatting for readability, but it is not yet the definitive version of record. This version will undergo additional copyediting, typesetting and review before it is published in its final form, but we are providing this version to give early visibility of the article. Please note that, during the production process, errors may be discovered which could affect the content, and all legal disclaimers that apply to the journal pertain.

© 2019 Published by Elsevier Masson SAS.

**Graphical abstract:**

# Synthesis and structure-activity relationship studies of $\alpha$ -naphthoflavone derivatives as CYP1B1 inhibitors

Jinyun Dong, Zengtao Wang, Jiahua Cui, Qingqing Meng\*, Shaoshun Li\*

\*School of Pharmacy, Shanghai Jiao Tong University, 800 Dongchuan Road, Shanghai, China. E-mail: [ssli@sjtu.edu.cn](mailto:ssli@sjtu.edu.cn) ; Fax: +86 021-34204775; Tel: +86 021-34204775

## Abstract

Cytochrome P450 1B1(CYP1B1) has been recognized as an important target for cancer prevention and reversing drug-resistance. In order to obtain potent and selective CYP1B1 inhibitors, a series of forty-one  $\alpha$ -naphthoflavone (ANF) derivatives were synthesized, characterized, and evaluated for CYP1B1, CYP1A1 and CYP1A2 inhibitory activities. A closure look into the structure-activity relationship for the inhibitory effects against CYP1B1 indicated that modification of the C ring of ANF would decrease the CYP1B1 inhibitory potency, while incorporation of substituent(s) into the different positions of the B ring yielded analogs with varying CYP1B1 inhibitory capacity. Among these derivatives, compounds **9e** and **9j** were identified as the most potent two selective CYP1B1 inhibitors with IC<sub>50</sub> values of 0.49 and 0.52 nM, which were 10-fold more potent than the lead compound ANF. In addition, Molecular docking and a reasonable 3D-QSAR (three-dimensional quantitative structure-activity relationship) study were performed to provide a better understanding the key structural features influencing the CYP1B1 inhibitory activity. The results achieved in this study would lay a foundation for future development of selective, potent, low-toxic and water-soluble CYP1B1 inhibitors.

**Key words:**  $\alpha$ -naphthoflavones, CYP1B1 inhibitors, SARs, 3D-QSAR

## 1. Introduction

Cytochrome P450 enzymes (CYPs) have been recognized as a large ubiquitous super-family of hemoprotein monooxygenases that are involved in a variety of reduction and oxidation reactions on both endogenic and xenobiotic compounds. Among them, CYP1 subfamily contains three members known as CYP1A1, CYP1A2, and CYP1B1. They are expressed in a tissue-specific manner: CYP1A1 and CYP1B1 are extrahepatic enzymes, while CYP1A2 is an intrahepatic enzyme. These three isoenzymes, particularly CYP1B1, are constitutively expressed in a wide variety of malignant tumors, such as the majority of mammary tumors, lung, and colon[1]. In fact, various planar aromatic molecules including 2,3,7,8-tetrachlorodibenzo-*p*-dioxin (TCDD) and 7,12-dimethylbenz[*a*]anthracene (DMBA) induce the overexpression of CYP1 enzymes via binding to the aryl hydrocarbon receptor (AhR), a ligand-activated transcription factor[2-5].

CYP1B1 enzyme has been extensively studied because of its predominant role in

metabolizing xenobiotics and endogenous compounds into carcinogenic forms and inducing drug resistance. A large number of pro-carcinogens such as exogenous polycyclic aromatic hydrocarbons (PAHs), polyhalogenated aromatic hydrocarbons (PHAHs), aryl and heterocyclic aryl amines as well as endogenous estrogens can be converted into cytotoxic, mutagenic and carcinogenic chemicals in presence of the overexpressed CYP1 enzymes[6]. Additionally, CYP1B1 can catalyze the 4-hydroxylation of 17 $\beta$ -estradiol (E<sub>2</sub>) subsequently leading to the formation of mutagenic E<sub>2</sub>-3,4-quinone that binds covalently to DNA. In contrast, CYP1A1 and CYP1A2 mediate hydroxylation of 17 $\beta$ -estradiol mainly to 2-hydroxyestradiol (2-OHE<sub>2</sub>), while its further-oxidized product E<sub>2</sub>-2,3-quinone is not considered carcinogenic[6]. Moreover, it should be noted that CYP1B1 can also metabolically inactivate a structurally diverse array of anti-cancer drugs such as docetaxel, tamoxifen, and paclitaxel, leading to drug resistance[7, 8]. All these findings suggest the clinical importance of CYP1B1 inhibitors in cancer prevention and treatment.

Recently, much emphasis has been on developing new and potent CYP1 inhibitors, and distinct families of chemicals containing flavonoids, trans-stilbenes, coumarins, alkaloids, and anthraquinone derivatives, have been characterized as CYP1 inhibitors[9, 10]. Among them,  $\alpha$ -naphthoflavone (ANF), also known as 7,8-benzoflavone, is one of the most potent CYP1 inhibitors. It exhibits strong inhibitory effects on recombinant human CYP1B1, CYP1A2, and CYP1A1 with IC<sub>50</sub> values of 5, 6 and 60 nM, respectively[11]. Evidence has accumulated during the past several years that ANF not only acts as a chemopreventive agent, but also enhances the sensitivity of CYP1B1-expressing cells to some anticancer drugs. Apart from its excellent biological activities, ANF also possesses a broad safety profile and health benefits[12]. All these promising properties indicate that ANF is an attractive anticancer drug for further study. Nevertheless, its further development is still restricted owing to its poor water solubility and very limited selectivity toward CYP1B1 over CYP1A2.

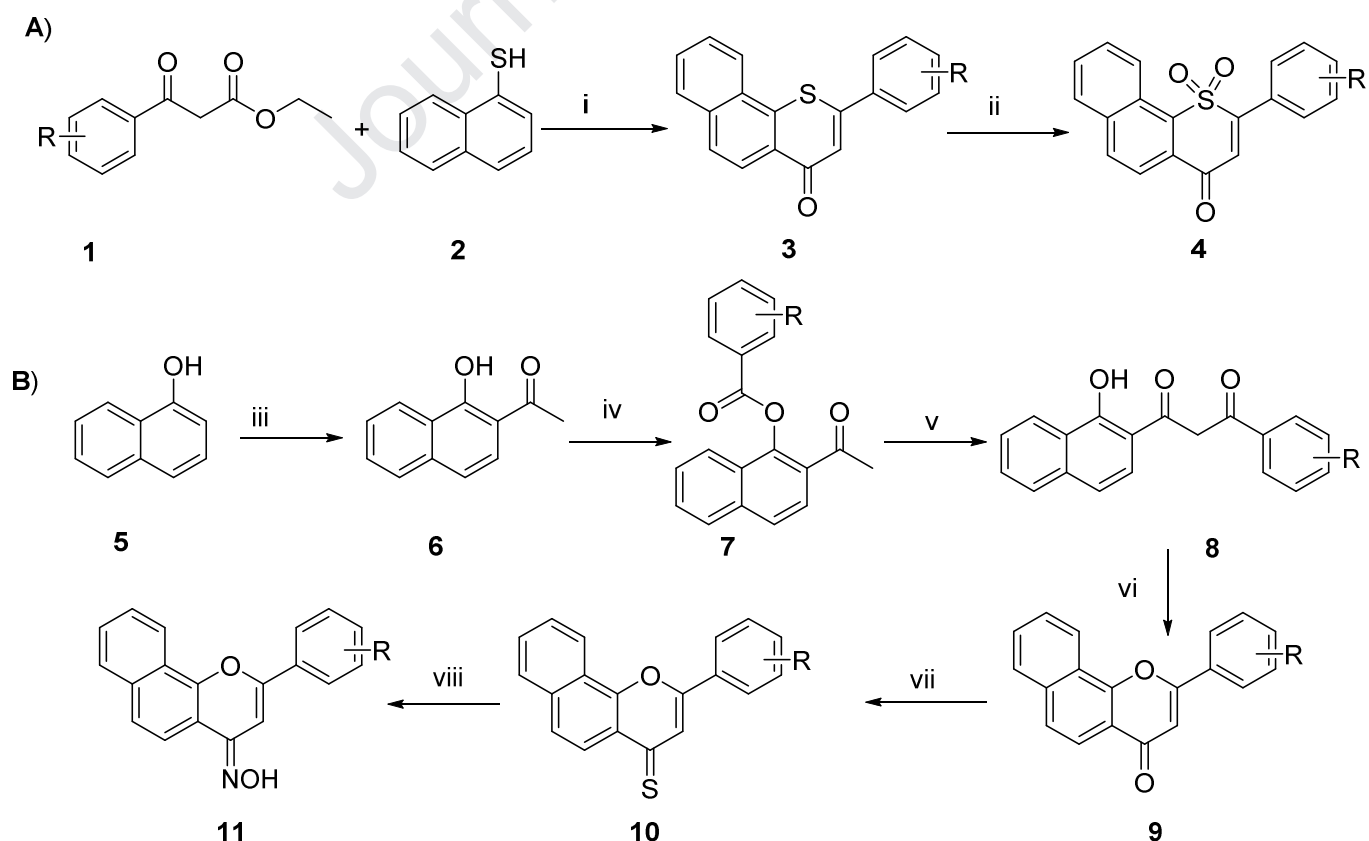
To address these problems, researchers including our research group have made great efforts to develop novel ANF derivatives, to the best of our knowledge, however, no such an ideal compound has ever been reported[13-16]. According to our previous results, we found that (1) introduction of hydrophobic and electron donor groups to the naphthalene moiety is beneficial for CYP1 inhibitory potency; (2) improvement of water solubility by reducing the C2-C3 double bond of ANF or introducing C3-hydroxyl group, or cleavage of the C ring of ANF results in a somewhat loss activity detrimental effect. Bearing in mind the above considerations, we consider that the B and C rings of ANF can be served as two additional sites for further modification and exploring the structure-activity relationships (SARs). As part of our continuous search for more potent and selective CYP1B1 inhibitors with improved water solubility, we synthesized various kinds of ANF derivatives.

## 2. Results and discussion

### 2.1 Chemistry

The synthetic routes adopted for the synthesis of ANF derivatives are illustrated in

Scheme 1A. The starting ethyl benzoylacetate derivatives **1** were synthesized from benzoic acid and ethyl potassium malonate according to reported method[15]. Commercially available naphthalene-1-thiol (**2**) was treated with ethyl benzoylacetate derivative **1** in the presence of polyphosphoric acid (PPA) at 120 °C to afford 2-substituted phenyl-4*H*-benzo[*h*]thiochromen-4-one derivatives **3a-e**, which were treated with 30% aqueous hydrogen peroxide solution in the presence of acetic acid at 60 °C to provide the corresponding 2-substituted phenyl-4*H*-benzo[*h*]thiochromen-4-one 1,1-dioxide derivatives **4a-b**[17]; ANF derivatives **9a-w**, **10a-h** and **11a-c** were synthesized as illustrated in Scheme 1B. Using Fries rearrangement reaction, acetylation of available naphthalen-1-ol (**5**) was carried out with acetic acid and ZnCl<sub>2</sub> at 120 °C to afford 1-(1-hydroxynaphthalen-2-yl)ethan-1-one (**6**) in good yields[18]. Intermediate **6** was further allowed to react with benzoic acid derivative in the presence of *N*-(3-dimethylaminopropyl)-*N'*-ethylcarbodiimide hydrochloride (EDCI) and 4-(dimethylamino)pyridine (DMAP) to give ester derivative **7**, which was treated with NaH to undergo Baker-Venkatarman rearrangement to yield 1-(1-hydroxynaphthalen-2-yl)-3-phenylpropane-1,3-dione derivative **8**. Intermediate **8** was further cyclized in the presence of H<sub>2</sub>SO<sub>4</sub>-EtOH solution (10%) at 90 °C to generate the 2-substituted phenyl-4*H*-benzo[*h*]chromen-4-one derivatives **9a-w**. The 2-substituted phenyl-4*H*-benzo[*h*]chromen-4-thione derivatives **10a-h** were next obtained by refluxing the corresponding flavone derivatives **9a-w** with Lawesson's reagent in dry toluene. Oximation of the corresponding 4-thioflavones **10a-h** by hydroxylamine hydrochloride in pyridine gave compounds **11a-c**.

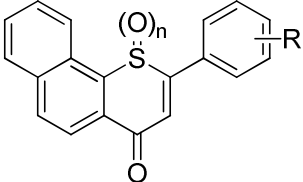


**Scheme 1. Reagents and conditions:** i) PPA, 120 °C; ii) H<sub>2</sub>O<sub>2</sub>, HOAc; iii) ZnCl<sub>2</sub>, HOAc; iv) benzoic acid derivative, EDCI, DMAP; v) NaH; vi) H<sub>2</sub>SO<sub>4</sub>-EtOH, 90 °C; vii) Lawesson's reagent, toluene, reflux; viii) hydroxylamine hydrochloride, Py, reflux. See **Tables 1-3** for the R group.

## 2.1 CYP1 enzyme inhibition activities

The synthesized compounds in this study were examined for their inhibitory effects on recombinant human CYP1 enzymes using the EROD (7-ethoxyresorufin O-deethylase) assay. Our previous study disclosed that replacement of the “O” atom at position-1 on the C-ring of ANF with a bioisosteric “NH” group caused a mild potency loss, indicating that a hydrophilic group would not be suitable for this substitution. Considering that sulfur atom is more lipophilic than oxygen atom, we converted this “O” atom at position-1 into a bioisosteric sulfur atom, intending to get novel compounds with modified biological behaviors. The results are presented in **Table 1**. Compounds **3a-e** showed moderate inhibitory activity toward CYP1B1, with decreased activity compared with that of ANF. Surprisingly, all of them displayed selective inhibition of CYP1A1 over CYP1B1 and CYP1A2. To verify whether the decreased inhibitory activities were caused by the relatively less electronegativity of sulfur atom, further oxidation of two potent CYP1B1 inhibitors **3a** and **3d** was carried out. However, a further decrease in CYP1B1 inhibitory activity was observed when a sulfone group was introduced at the 1-position (compounds **4a** and **4b**) in comparison to the corresponding sulfur-substituted forms. Based on these data, we can conclude that the oxygen atom at this site in ANF is very important for achieving high affinity for ligand binding, although it does not appear to be making any interactions with any amino acid residue in the crystal structure of ANF bound to CYP1B1.

**Table 1** Inhibitory activities of sulfur substituted  $\alpha$ -naphthoflavones on CYP1 enzymes



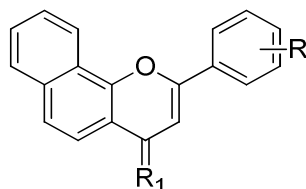
Compd.	n	R	IC <sub>50</sub> values (nM)			IC <sub>50</sub> ratio	
			1B1	1A1	1A2	1A1/1B1	1A2/1B1
<b>3a</b>	0	H	57.0	32.6	>1000	0.6	>17.5
<b>3b</b>	0	<i>o</i> -F	103.6	84.6	582.2	0.8	5.6
<b>3c</b>	0	<i>o</i> -Cl	89.7	45.8	>1000	0.5	>11.1
<b>3d</b>	0	<i>m</i> -Cl	40.5	13.6	295.8	0.3	7.3
<b>3e</b>	0	<i>p</i> -Cl	51.9	9.0	211.9	0.2	4.0
<b>4a</b>	2	H	222.9	129.2	169.6	0.6	0.8
<b>4b</b>	2	<i>m</i> -Cl	250.4	>1000	698.7	>4.0	2.8

Compd.	n	R	IC <sub>50</sub> values (nM)			IC <sub>50</sub> ratio	
			1B1	1A1	1A2	1A1/1B1	1A2/1B1
ANF	-	-	5.9	80.3	18.0	13.6	3.1

Similarly, we turned our attention to the C4-position of ANF to confirm whether modification at this position could provide more potent CYP1B1 inhibitors. As a general trend, replacement of the oxygen atom at C4-position of ANF with a sulfur atom led to compounds **10a-h**, which exhibited more potent CYP1B1 inhibitory activity in comparison with that of substitution at 1- oxygen atom as shown in **Table 2**. Among them, compounds **10a**, **10c**, **10d**, **10e**, and **10g** possessed single digit nanomolar IC<sub>50</sub> values toward CYP1B1 (IC<sub>50</sub> values of 7.8, 5.0, 9.4, 9.1 and 1.6 nM, respectively). Of particular note, although most of them were identified as potent CYP1B1 inhibitors, only compound **10g** showed a 3-fold improvement in the CYP1B1 biochemical assay when compared with ANF. Therefore, we speculate that substitution with a sulfur atom at this site may have a very limited potential for improving CYP1B1 inhibitory efficiency.

Next, compounds **11a-c** were designed by oximation of the corresponding representative compounds **10a**, **10d**, and **10g** for the following reasons: (1) as a hydrogen bond acceptor and donor, oxime group may form hydrogen bond interactions with some residues; (2) oxime group can be metabolized by CYP1B1, indicating that oxime-containing derivatives may have high affinity for ligand binding; (3) hydrophilic oxime group not only contributes to improving water solubility, but also provides reaction site for further modification. We evaluated the newly designed oxime-containing derivatives **11a-c** and found that they still showed similar CYP1B1 inhibitory activities with IC<sub>50</sub> values ranging from 3.2 to 10.4 nM. In this respect, compound **11a** was slightly more active than ANF in CYP1B1 inhibition, while introduction of a substituent to the B-ring (compounds **11b** and **11c**) diminished its CYP1 inhibitory activity. Together with these findings, it is implied that modification at C4-position generally had a slight effect in improving inhibitory efficiency toward CYP1B1, whereas had a most pronounced effect in their selectivity. Compared with ANF, all of these compounds displayed an increased selectivity between CYP1B1 and CYP1A2, but a decreased selectivity between CYP1B1 and CYP1A1.

**Table 2** Inhibitory activities of C4 sulfur/oxime substituted  $\alpha$ -naphthoflavones on CYP1 enzymes



Compd.	R <sub>1</sub>	R	IC <sub>50</sub> values (nM)			IC <sub>50</sub> ratio	
			1B1	1A1	1A2	1A1/1B1	1A2/1B1
<b>10a</b>	S	H	7.8	65.4	179.0	8.4	22.9



Compd.	R <sub>1</sub>	R	IC <sub>50</sub> values (nM)			IC <sub>50</sub> ratio	
			1B1	1A1	1A2	1A1/1B1	1A2/1B1
<b>10b</b>	S	<i>o</i> -F	10.6	31.9	51.8	3.0	4.9
<b>10c</b>	S	<i>m</i> -F	5.0	25.1	134.1	5.0	26.8
<b>10d</b>	S	<i>m</i> -Cl	9.4	31.7	304.2	3.4	32.4
<b>10e</b>	S	<i>m</i> -OCH <sub>3</sub>	9.1	72.8	304.7	8.0	33.5
<b>10f</b>	S	<i>p</i> -F	13.3	12.3	42.8	0.9	3.2
<b>10g</b>	S	<i>p</i> -Cl	1.6	9.6	53.2	6.0	33.3
<b>10h</b>	S	3,4,5- <i>tri</i> OCH <sub>3</sub>	18.8	28.2	>1000	1.5	>53.2
<b>11a</b>	=N-OH	H	3.2	32.1	74.6	10.0	23.3
<b>11b</b>	=N-OH	<i>m</i> -Cl	10.4	94.9	803.6	9.1	77.3
<b>11c</b>	=N-OH	<i>p</i> -Cl	8.0	44.4	75.2	5.6	9.4
<b>ANF</b>	-	-	5.9	80.3	18.0	13.6	3.1

From the above observations, it can be reasonably concluded that oxygen atoms at positions 1 and 4 of ANF are important for CYP1B1 inhibitory activity, so it seems to be very hard to obtain a compound with significantly increased CYP1B1 inhibitory activity by replacement of these two oxygen atoms. Analysis of the crystal structure of CYP1B1 in complex with ANF showed that the phenyl ring (B ring) of ANF comes into close contact with heme[19]. As a result, introduction of substituents to the phenyl ring may affect the formation of the reactive heme iron-oxo intermediate during catalysis. Based on this idea, we therefore turned our attention to the phenyl ring of ANF. As shown in **Table 3**, at the start of this study, synthesis and evaluation of halogen- and methoxyl-substituted ANF analogs **9a-h** was intended to identify the optimum location on the phenyl moiety. There was an increase in potency against CYP1B1 and CYP1A1, while a decrease in potency against CYP1A2 for most of the substituted derivatives when compared to the unsubstituted parent compound ANF. In particular, a significant increase in CYP1B1 inhibitory activity was observed when a chlorine atom was introduced at the *meta*-position (compound **9e**). This compound showed an IC<sub>50</sub> value of 0.49 nM, which was a 12-fold increase over lead compound ANF (IC<sub>50</sub> value of 5.9 nM). Furthermore, **9e** displayed a significantly increased selectivity toward CYP1B1 over CYP1A2 when compared to ANF (150.2 vs 3.1). However, to our surprise, moving this chlorine atom from the *meta*- to *ortho*-position led to a significant loss in CYP1 inhibitory potency. Analysis of the biological data of compounds **9a-c** (F derivatives), **9d-f** (Cl derivatives) and **9g-h** (OCH<sub>3</sub> derivatives), we can preliminarily conclude that *meta*-position was optimal for substitution on the phenyl ring.

Next, *meta*-substituted compounds **9i-k** were synthesized in order to explore the effect of hydrophilic/lipophilic groups on the CYP1 inhibitory activity. Among them, compound **9j** bearing a lipophilic “CF<sub>3</sub>” group was identified as the most potent



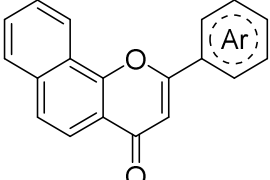
CYP1B1 inhibitors with  $IC_{50}$  value of 0.52 nM, which was equipotent to the *meta*-chlorine substituted derivative **9e**. Dimethylamino substituted derivative **9k** showed a similar level of CYP1B1 inhibitory activity to ANF, while a hydrophilic group of hydroxyl **9i** resulted in a nearly 3-fold decrease in activity ( $IC_{50}$  = 14.8 nM), suggesting that lipophilic group(s) may be beneficial for CYP1B1 inhibitory activity. Compared with *meta*-fluorine substituted compound **9b**, *meta*-trifluoromethyl substituted derivative **9j** was found to be 4-fold more potent in blocking CYP1B1 activity. Based on this observation, we hypothesized that introduction of more lipophilic groups to the phenyl ring may increase their inhibitory activity toward CYP1B1. Thus, compounds **9l-o** bearing lipophilic groups both at *meta*-position and other position(s) were synthesized. However, it was found that, compared to **9e** or **9j**, all of these multi-substituted derivatives exhibited a slight decrease in CYP1B1 inhibitory potency with  $IC_{50}$  values ranging from 3.2 to 5.6 nM. The positive correlation between lipophilicity and biochemical activity was not observed, indicating that steric hindrance may be an important factor in blocking CYP1 enzymes. To test our hypothesis, a larger naphthalene ring was introduced to give compound **9p**. As expected, compared with ANF, a significantly decreased potency in blockage of CYP1B1 and CYP1A2 was observed for compound **9p** with  $IC_{50}$  values of 48.4 and more than 1000 nM, respectively, supporting our hypothesis.

As we all know, ANF has quite low water solubility owing to its planar and hydrophobic structure, which limits its application range. Although our above results pointed to the importance of lipophilicity on CYP1B1 inhibitory activity, we still want to introduce some hydrophilic functional groups to improve its water solubility. Thus, nitrogen-containing compounds **9q-t** were prepared since hydrophilic piperazine and morpholine groups have been widely recognized as ‘privileged scaffolds’ in medicinal chemistry. Derivative **9r** incorporated with a 4-methyl-piperazin-1-yl group at the *meta*-position of phenyl ring showed more potent than *para*-substituted analogue **9q** on inhibition of CYP1B1 ( $IC_{50}$  values of 24.6 and 63.8 nM, respectively), which is in agreement with our previous results. Addition of a chlorine atom to the *meta*-position of **9r** affording analogue **9s** resulted in a 2-fold decrease in  $IC_{50}$  value from 24.6 to 47.7 nM for CYP1B1 inhibition, however, replacement of the 3-(4-methyl-piperazin-1-yl) group of **9r** with a 4-morpholinyl group giving analogue **9t**, led to a 12-fold increase in  $IC_{50}$  value from 24.6 to 2.0 nM against CYP1B1. Therefore, we speculated that the enhanced CYP1B1 inhibitory activity of compound **9t** may be partly due to the reduced steric hindrance. Of particular note, CYP1A2 enzyme appears to be even more sensitive to steric hindrance than CYP1B1 according to the relationship between structural features of compounds **9n-t** and biological activities of CYP1A2 inhibition ( $IC_{50}$  values ranging from submicromolar to micromolar levels). It may be ascribed to the smallest active site cavity volume of CYP1A2 among CYP1 family members[19-21]. For the purpose of improving its water solubility, physiologically acceptable salts of piperazine substituted ANF derivative **9q** were prepared by adding different kinds of acids. To our surprise, the sulfate form of compound **9q** exhibited a significantly increased water solubility (more than 20 mg/ml). However, in the subsequent experiment of reversing CYP1B1

induced drug-resistance, we found this compound also displayed a remarkable cytotoxicity towards MCF-7 breast cancer cells when compared with ANF. We speculate that its enhanced cytotoxicity may be associated with the piperazinyl group on the B ring.

Given that an ideal ANF derivative with improved CYP1B1 inhibitory activity and water solubility cannot be obtained by introduction of nitrogen-containing aliphatic heterocycle to the phenyl ring of ANF, we attempted to replace this phenyl ring with alkaline pyridine ring (analogues **9u-w**), which can be used for further modification to improve water solubility. To our surprise, compounds **9u-w** showed that pyridine substitution was tolerated with slight increase or only minimal loss of CYP1B1 inhibitory activity as compared with ANF. With regard to this series, 2-pyridine derivative **9u** was found to be the most potent CYP1B1 inhibitor with  $IC_{50}$  value of 3.5 nM, while 2- and 3-pyridine derivatives **9v** and **9w** were slightly less active at 6.2 and 9.3 nM, respectively, suggesting the importance of the position of nitrogen atom in CYP1 inhibitory potency. It should be noted that compared with ANF, these three compounds also exhibited an enhanced inhibitory activity toward CYP1A1, but a decreased inhibitory activity toward CYP1A2, which contributes to improving the selectivity between CYP1B1 and CYP1A2. Based on this finding, it could be envisaged that some other aromatic heterocycles may also be tolerated for the B ring of ANF, and significantly affect their inhibitory activity toward CYP1 isoenzymes. Moreover, their cytotoxicity was not significantly augmented by replacing the phenyl ring with nitrogen-containing aromatic heterocycle as compared to ANF, suggesting the great potential of B ring in structural modification.

**Table 3** Inhibitory activities of B ring modified  $\alpha$ -naphthoflavones against CYP1s



Compd.	Ar	$IC_{50}$ values (nM)			$IC_{50}$ ratio	
		1B1	1A1	1A2	1A1/1B1	1A2/1B1
<b>ANF</b>	-	5.9	80.3	18.0	13.6	3.1
<b>9a</b>	2-fluorophenyl	3.3	12.2	23.7	3.7	7.2
<b>9b</b>	3-fluorophenyl	2.2	16.7	62.2	7.6	28.3
<b>9c</b>	4-fluorophenyl	2.7	6.7	12.1	2.5	4.5
<b>9d</b>	2-chlorophenyl	21.6	227.9	113.2	10.6	5.2
<b>9e</b>	3-chlorophenyl	0.49	5.2	73.6	10.6	150.2
<b>9f</b>	4-chlorophenyl	4.2	4.3	10.6	1.0	2.5
<b>9g</b>	3-methoxyphenyl	3.8	35.8	177.8	9.4	46.8

Compd.	Ar	IC <sub>50</sub> values (nM)			IC <sub>50</sub> ratio	
		1B1	1A1	1A2	1A1/1B1	1A2/1B1
<b>9h</b>	4-methoxyphenyl	7.3	30.9	98.2	4.2	13.5
<b>9i</b>	3-hydroxyphenyl	14.8	53.1	91.5	3.6	6.2
<b>9j</b>	3-(trifluoromethyl)phenyl	0.52	16.7	94.2	32.1	181.2
<b>9k</b>	3-(dimethylamino)phenyl	4.1	9.6	183.3	2.3	44.7
<b>9l</b>	3,5-dichlorophenyl	4.2	25.5	156.9	6.1	37.4
<b>9m</b>	3,4-difluorophenyl	5.6	11.8	28.6	2.1	5.1
<b>9n</b>	3,4,5-trimethoxyphenyl	5.1	3.0	>1000	0.6	>196.1
<b>9o</b>	3-chloro-5-methoxyphenyl	3.2	163.9	>1000	51.2	312.5
<b>9p</b>	2-naphthyl	48.4	46.4	>1000	1.0	>20.7
<b>9q</b>	4-(4-methyl-piperazin-1-yl) phenyl	63.8	153.4	>1000	2.4	15.7
<b>9r</b>	3-(4-methyl-piperazin-1-yl) phenyl	24.6	34.6	761.6	1.4	31.0
<b>9s</b>	3-Cl-5-(4-methyl-piperazin-1-yl) phenyl	47.7	37.9	>1000	0.8	21.0
<b>9t</b>	3-(4-morpholinyl)phenyl	2.0	30.9	318.5	15.5	159.3
<b>9u</b>	2-pyridyl	3.5	37.9	25.1	10.8	7.2
<b>9v</b>	3-pyridyl	6.2	25.3	23.2	4.1	3.7
<b>9w</b>	4-pyridyl	9.3	18.7	36.4	2.0	3.9

## 2.2 Molecular docking

To gain insight into the potential binding modes and rationalize the observed efficiency and selectivity of CYP1 inhibition by the most potent CYP1B1 inhibitor **9e**, we performed a molecular docking study based on the crystal structures of CYP1B1 or CYP1A2 in complex with ANF (PDB IDs of 3PM0 and 2HI4, respectively). As can be seen from part A of **Figure 1**, similar to ANF, compound **9e** tightly fitted well into the active sites of both CYP1B1 and CYP1A2, while it adopted a different binding pose to ANF within the corresponding ligand binding pocket. ANF forms only one hydrogen bond to Asp326 of CYP1B1 with a distance of 2.8 Å. However, the carbonyl group of compound **9e** could form three hydrogen bonds to the amino and hydroxyl groups of Ser131 as well as the carbonyl group of Asp326 with distances of 3.5, 2.1 and 2.8 Å, respectively, which may play an essential role in improving its binding affinity to CYP1B1 (Figure 1B). In addition to the common  $\pi$ - $\pi$  stacking interaction formed by naphthalene part and phenyl ring of Phe231, the T-shaped  $\pi$ - $\pi$  stacking interaction between the phenyl moiety provided an additional binding affinity. Also, compound **9e** is

buried in hydrophobic contacts with the residues such as Leu264, Phe268, Phe120, Ala330 and Ala121. The presence of a chlorine atom not only affected the binding pose of **9e** in CYP1B1, but also provide an extra hydrophobic contact with Ile399. All of these factors could contribute to the improvement in the enzyme inhibition activity of CYP1B1. However, in the case of compound **9e** bound to CYP1A2 (Figure 1D), the most significant difference between **9e** and ANF is that no hydrogen bond or water-mediated hydrogen bond was formed between compound **9e** and CYP1A2 (ANF could form a water-mediated hydrogen bond with Gly316<sup>[20]</sup>). As a result, the binding affinity of **9e** for CYP1A2 arises mainly from a  $\pi$ - $\pi$  stacking interaction with Phe226 and hydrophobic contacts with many hydrophobic residues such as Val227, Phe226, Phe260, Thr498, Leu382, Ile386, Thr321 and Ala317. This observation may provide a reasonable explanation for a lower activity of compound **9e** against CYP1A2.

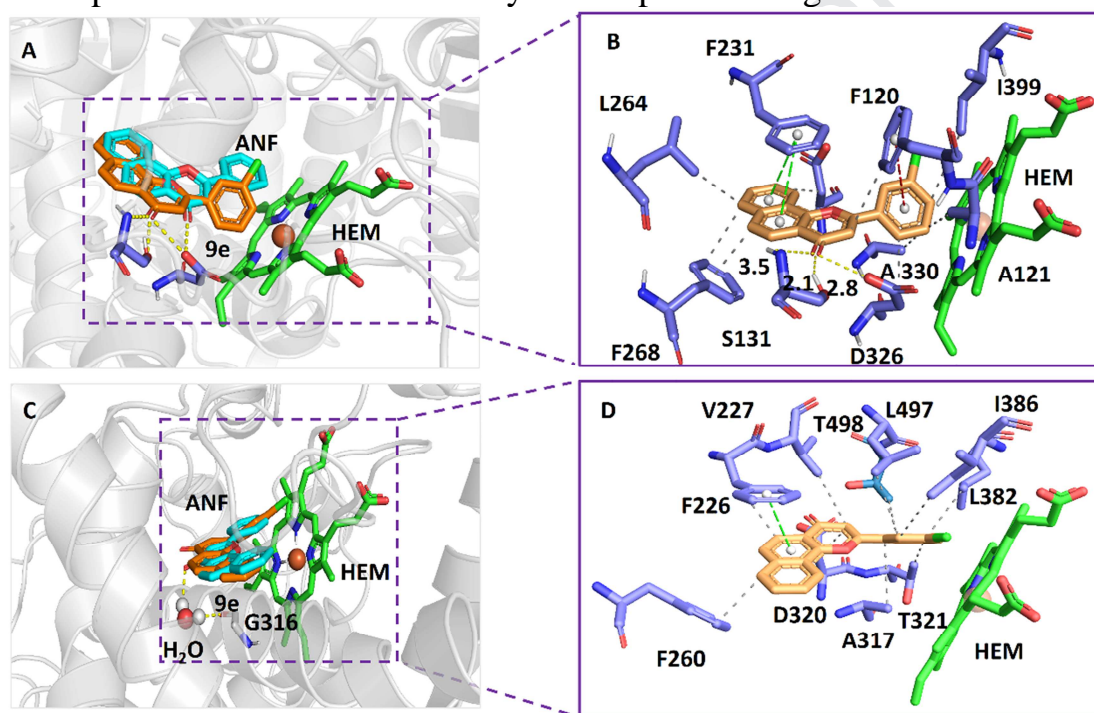


**Figure 1** The binding models of compound **9e** with CYP1B1(A) and CYP1A2 (C). (Hydrogen bonding is depicted by yellow dashed lines;  $\pi$ - $\pi$  stacking interaction is depicted by green dashed lines; T-shaped  $\pi$ - $\pi$  stacking interaction is depicted by red dashed lines; and, hydrophobic contacts is depicted by grey dashed lines. In parts A and C, ANF was shown in cyan, while **9e** was shown in yellow )

### 2.3 3D-QSAR study

In the current work, 3D-QSAR (three-dimensional quantitative structure-activity relationship) models CoMFA (comparative molecular field analysis) and CoMSIA (comparative molecular similarity indices analysis) studies were undertaken to figure out the effects of steric, electrostatic, hydrophobic, and hydrogen bonding properties of these compounds on CYP1B1 inhibitory activity, and to obtain reliable models to predict the inhibitory activity of structurally similar compounds on CYP1B1. Based on the variety of activity and structure diversity, all the forty-two compounds were divided into a training set comprising 33 compounds and an external test set comprising nine

compounds: the test set consists of compounds **10d**, **3b**, **4b**, **9a**, **9e**, **9k**, **9m**, **9w** and ANF; the remaining compounds were used as training set. Molecular alignment of compounds is a crucial step in the development of 3D-QSAR model. Compound **9j**, one of the most active molecule, was chosen as the template molecule and all the other molecules were aligned to it using the database alignment method in SYBYL-X 2.0. The aligned molecules are shown in **Figure 2**.

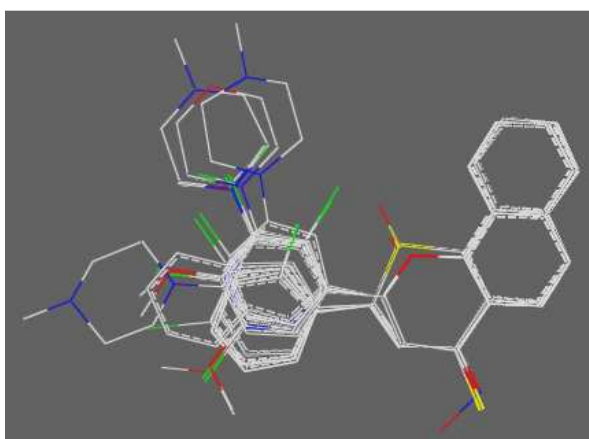


**Figure 2** Database alignment superposition of training set used for 3D-QSAR analysis based on compound **9j**.

Based on the molecular alignment, CoMFA and CoMSIA were applied to derive a correlation relationship between the CYP1B1 inhibitor biological activity and the structural properties. A partial least squares (PLS) approach was used to derive the 3D-QSAR model. Initial CoMFA PLS analysis with all 33 compounds in the training set afforded model with very low cross-validated  $q^2$  value. After omitting four possible outliers, compounds **10g**, **11b**, **9i** and **9r**, a better  $q^2$  value of 0.526 was obtained from a training set of 29 compounds. Meanwhile, the corresponding conventional correlation coefficient  $r^2$ , standard error of the estimate (SEE), and the variance ratio  $F(n_1=6, n_2=22)$  were also calculated as 0.981, 0.094 and 191.581, respectively. The  $IC_{50}$  values of these ANF derivatives were predicted to validate the stability and predictive ability of CoMFA model. As shown in **Figure 3** and **Table 4**, the predicted values were in good agreement with the experimental data for the training set indicated the reliability of CoMFA model. Also, this figure shows a good agreement between experimental and predicted values for the test set within a statistically tolerable error range.

**Table 4** Experimental and predictive activities of CoMFA for the 38  $\alpha$ -naphthoflavone analogues.

Compd.	$pIC_{50}$		Residual	Compd.	$pIC_{50}$		Residual
	Actual	Predicted			Actual	Predicted	
<b>10a</b>	8.108	8.105	0.003	<b>9d</b>	7.666	7.923	-0.257
<b>10b</b>	7.975	7.902	0.073	<b>9e<sup>#</sup></b>	9.31	8.872	0.438
<b>10c</b>	8.301	8.375	-0.074	<b>9f</b>	8.377	8.32	0.057
<b>10d<sup>#</sup></b>	8.027	8.316	-0.289	<b>9g</b>	8.42	8.498	-0.078



Compd.	pIC <sub>50</sub>		Residu	Compd.	pIC <sub>50</sub>		Residual
<b>10e</b>	8.041	8.091	-0.05	<b>9h</b>	8.137	8.179	-0.042
<b>10f</b>	7.876	7.912	-0.036	<b>9j</b>	9.284	9.231	0.053
<b>10h</b>	7.726	7.771	-0.045	<b>9k<sup>#</sup></b>	8.387	8.867	-0.48
<b>11a</b>	8.495	8.377	0.118	<b>9l</b>	8.377	8.313	0.064
<b>11c</b>	8.097	8.165	-0.068	<b>9m<sup>#</sup></b>	8.252	8.597	-0.345
<b>3a</b>	7.244	7.273	-0.029	<b>9n</b>	8.292	8.229	0.063
<b>3b<sup>#</sup></b>	6.985	7.209	-0.224	<b>9o</b>	8.495	8.54	-0.045
<b>3c</b>	7.047	7.109	-0.062	<b>9p</b>	7.315	7.21	0.105
<b>3d</b>	7.393	7.339	0.054	<b>9q</b>	7.195	7.126	0.069
<b>3e</b>	7.285	7.282	0.003	<b>9s</b>	7.321	7.294	0.027
<b>4a</b>	6.652	6.654	-0.002	<b>9t</b>	8.699	8.705	-0.006
<b>4b<sup>#</sup></b>	6.601	6.966	-0.365	<b>9u</b>	8.456	8.329	0.127
<b>9a<sup>#</sup></b>	8.481	8.142	0.339	<b>9v</b>	8.208	8.338	-0.13
<b>9b</b>	8.658	8.65	0.008	<b>9w<sup>#</sup></b>	8.032	8.273	-0.241
<b>9c</b>	8.569	8.468	0.101	<b>ANF<sup>#</sup></b>	8.229	8.24	-0.011

<sup>#</sup> represents the test set compounds

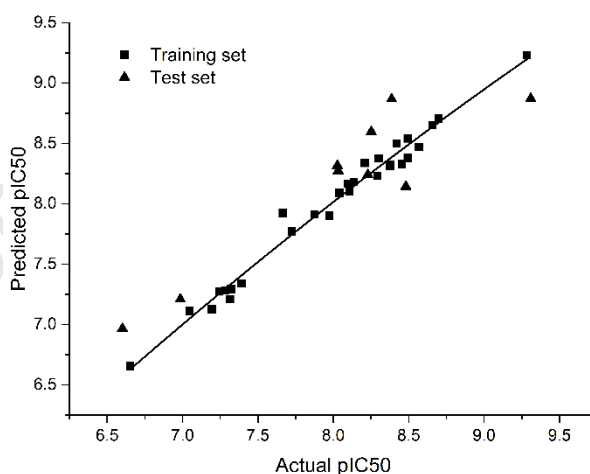


**Figure 3** Correlation plot of the predicted pIC<sub>50</sub> with the experimental pIC<sub>50</sub> values generated through CoMFA .

CoMFA and CoMSIA contour maps can be applied to rationalize the regions in 3D space around the molecules where changes in the particular physicochemical properties are predicted to increase or decrease the activity. In general, the molecular force field of the CoMFA model includes the steric and electrostatic fields. However, in our CoMFA study, no electrostatic contour map was found, and only the steric contour map was generated with **9j** as a reference structure (**Figure 4**), indicating that the interaction of steric field is extremely important for potency (the contribution of steric is 100%). The steric interaction is denoted by green and yellow contours. A large green contour near the

meta-position of the benzene ring indicates that a bulky substituent at this site would increase the CYP1B1 inhibitory potency. This is consistent with the fact that most compounds bearing substituents at meta position of the benzene ring generally showed an enhanced CYP1B1 inhibitory activity. Inversely, a small yellow contour near the ortho-position of the benzene ring means that steric bulk is unfavored at this site. Consistent to our experimental results, ortho-substituted derivatives generally showed a decreased CYP1B1 inhibitory activity when compared with meta- or para-substituted analogs. Similarly, the presence of a yellow contour around the 1-position oxygen atom of C ring indicates this site is a disfavored region for steric bulk and replacement of this oxygen atom with other groups (such as sulfur and sulfone groups) should be avoided in future design.

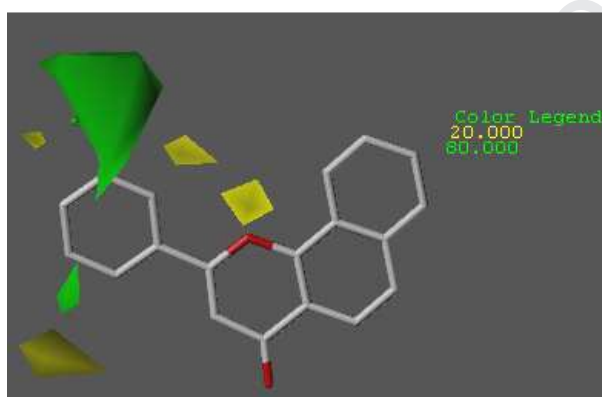


**Figure 4** The steric contour map of CoMFA for  $\alpha$ -naphthoflavone analogues.

Considering that CoMSIA model, including five molecular force fields (steric, electrostatic, hydrophobic, hydrogen bond donor, and hydrogen bond acceptor fields), could provide a more comprehensive understanding of the key structural requirements responsible for the biological activity. Using the similar method mentioned above, we also established a reasonable CoMSIA model with satisfactory statistical values including  $q^2$ ,  $r^2$ , and SEE values (0.598, 0.937, and 0.179, respectively). It should be noted that the training set for CoMSIA model consists of 34 compounds, and the remaining eight compounds are test set (**10g**, **11a**, **9e**, **9i**, **9u**, **9v**, **9w** and ANF). The relative field contributions of the hydrophobic, hydrogen bond acceptor, steric and electrostatic fields were 27.4, 38.7, 8.6 and 25.2%, respectively, suggesting that hydrophobic, hydrogen bond acceptor and electrostatic interactions play relatively more important roles in the CYP1B1 inhibitory activity. The contour maps for CoMSIA are depicted in **Figure 5**. A prominent magenta colored contour near the carbonyl oxygen atom indicates that a hydrogen bond acceptor is favored at this position (**Figure 5a**). The red contours present near 1-position oxygen atom shows unfavorable activity for the presence of a hydrogen bond acceptor group. In **Figure 5b**, the hug yellow contour surrounding the phenyl ring reflects the increase in activity found by introducing hydrophobic group in this region. Seen from **Figure 5c**, the phenyl moiety is surrounded by a large red contour, which means that electron-withdrawing increase the activity



substituent in this region is beneficial to the activity. A green contour centralizes on the meta-position of the phenyl ring reveals around this region bulky substituent is favored (Figure 5d), which is also in consistent with the above mentioned CoMFA steric field. In addition, a yellow contour was also found around this phenyl ring suggesting the existence of multiple substituents at the phenyl ring is unfavorable for CYP1B1 inhibitory activity.

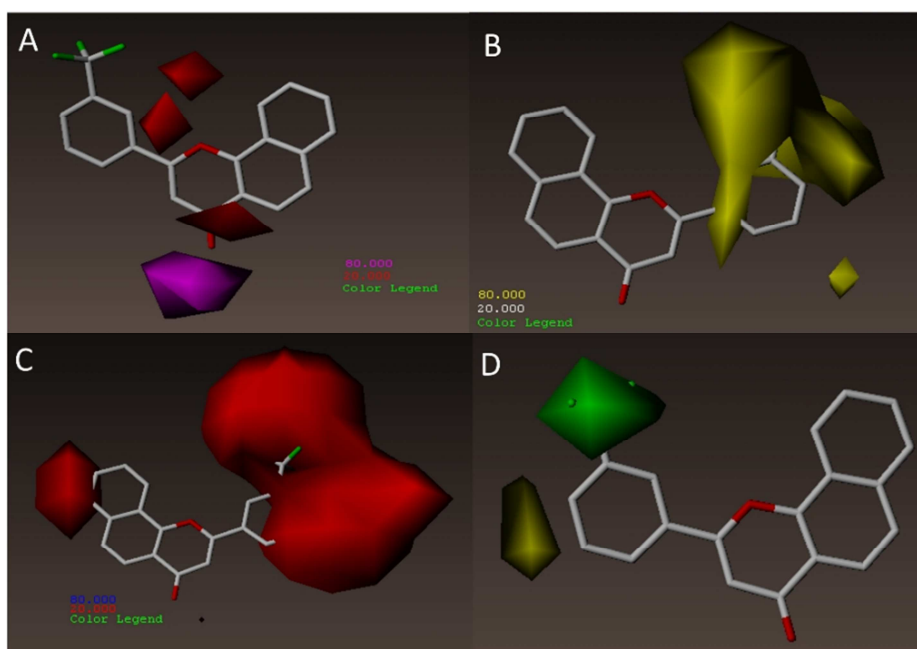


**Figure 5** Contour maps of CoMSIA model: hydrogen-bond acceptor field (A), hydrophobic field (B), electrostatic field (C), and steric field (D).

### 3 Conclusion

In this study, structural modification of ANF gave a series of forty-one derivatives, which exhibited varied levels of inhibitory potencies on CYP1B1, CYP1A1 and CYP1A2 enzymes. Among them, compounds **9e** and **9j** were found to be the most potent two CYP1B1 inhibitors with  $IC_{50}$  values of 0.49 and 0.52 nM, which were 10-fold more potent than the lead compound ANF. Meanwhile, these two compounds also presented an enhanced selectivity for inhibition of CYP1B1 over CYP1A2. To rationalize the biological results and gain more information on the binding mode of these compounds, a molecular docking study was performed and the result revealed that the hydrogen bond and hydrophobic interactions are two important factors for increasing the binding affinity at CYP1B1 active site. To get enough information for better understanding the structure-activity relationship and the key structural features influencing the activity, a 3D-QSAR study on CYP1B1 inhibition was also conducted. The reasonable CoMFA and CoMSIA models showed satisfactory correlations and predictive abilities. Their contour maps emphasized the importance of oxygen atom at 1 position, carbonyl oxygen atom at 4 position, as well as hydrophobic and electron-withdrawing substituent at meta-position of the phenyl ring for CYP1B1 inhibitory activity. Based on the observation that

variation of the phenyl ring of ANF has a significant impact on the CYP1 inhibitory activity and aromatic heterocycles are also well tolerated for this part, we have successfully developed many derivatives with more potent inhibition of CYP1B1, high selectivity and improved aqueous solubility by expanding the phenyl and naphthyl, and they will be reported in due course.

## 4. Experimental

### 4.1. Chemistry

All starting materials and reagents were either obtained from commercial suppliers or prepared according to literature reported procedures. All purchased chemicals and solvents were used without further purification unless otherwise indicated. All anhydrous solvents were dried according to standard methods. Column chromatography was conducted on silica gel (200-300 mesh) from Qingdao Ocean Chemical Factory. The  $^1\text{H}$  and  $^{13}\text{C}$  NMR spectra were obtained on a Varian Mercury-300 (400 MHz) spectrometer using  $\text{DMSO-}d_6$  and  $\text{CDCl}_3$  as solvents and TMS as an internal standard. All chemical shifts ( $\delta$ ) are given in ppm and coupling constants are given in Hz. Reactions progress was monitored by thin-layer chromatography TLC (silica gel GF254) and visualized with UV light (254 or 365 nm). Mass spectra were recorded with HRMS (ESI, Agilent 6540 QTOF).

#### 4.1.1 General procedure for the preparation of 2-substituted phenyl-4H-benzo[h]thiochromen-4-one derivatives **3a-e**

Ethyl benzoylacetate derivative **1** was prepared according to reported methods[15]. A mixture of commercially available naphthalene-1-thiol (**2**, 1 equivalent), ethyl benzoylacetate derivative **1** (2 equivalents), and polyphosphoric acid (PPA) was heated at 120 °C with stirring. After the reaction was completed, the mixture was cooled to room temperature and neutralized with NaOH aqueous. Then, the resulting mixture was extracted with EtOAc. The combined organic extracts were washed with saturated NaCl aqueous, dried over  $\text{Na}_2\text{SO}_4$  and the solvent removed under vacuum. The crude residue was subjected to silica gel column chromatography to give compounds **3a-e**.

4.1.1.1 2-phenyl-4H-benzo[h]thiochromen-4-one (**3a**). Pale white solid, yield: 58%;  $^1\text{H}$  NMR (400 MHz,  $\text{DMSO-}d_6$ )  $\delta$  8.54 (d,  $J = 7.2$  Hz, 1H), 8.38 (d,  $J = 8.7$  Hz, 1H), 8.24 – 8.08 (m, 2H), 8.02 – 7.90 (m, 2H), 7.88 – 7.77 (m, 2H), 7.71 – 7.57 (m, 3H), 7.43 (s, 1H).  $^{13}\text{C}$  NMR (101 MHz,  $\text{CDCl}_3$ )  $\delta$  181.01, 151.13, 137.26, 136.67, 133.99, 130.77, 129.56, 129.46, 129.30, 128.99, 128.94, 127.94, 127.30, 127.12, 124.08, 123.78, 123.56. HRMS (ESI) calcd for  $[\text{C}_{19}\text{H}_{12}\text{SO} + \text{H}]^+$  289.0687, found 289.06861.

4.1.1.2 2-(2-fluorophenyl)-4H-benzo[h]thiochromen-4-one (**3b**). Pale white solid, yield: 55%;  $^1\text{H}$  NMR (400 MHz,  $\text{CDCl}_3$ )  $\delta$  8.47 (d,  $J = 8.5$  Hz, 1H), 8.29 (d,  $J = 7.9$  Hz, 1H), 7.86 (t,  $J = 9.5$  Hz, 2H), 7.69 – 7.51 (m, 3H), 7.43 (s, 1H), 7.29 – 7.18 (m, 3H).  $^{13}\text{C}$  NMR (101 MHz,  $\text{CDCl}_3$ )  $\delta$  180.65, 149.18, 145.08 (d,  $J = 2.0$  Hz), 137.63, 133.96, 132.16, 132.08, 130.28 (d,  $J = 2.0$  Hz), 129.48, 129.32, 129.00 (d,  $J = 2.0$  Hz), 128.02, 127.48 (d,  $J = 4.0$  Hz), 127.32, 124.78 (d,  $J = 4.0$  Hz), 123.76, 123.52, 116.88, 116.66. HRMS (ESI) calcd for  $[\text{C}_{19}\text{H}_{11}\text{FSO} + \text{H}]^+$  307.0593, found 307.05954.

**4.1.1.3 2-(2-chlorophenyl)-4H-benzo[h]thiochromen-4-one (3c).** Pale white solid, yield: 48%;  $^1\text{H}$  NMR (400 MHz,  $\text{CDCl}_3$ )  $\delta$  8.47 (d,  $J = 8.6$  Hz, 1H), 8.23 (d,  $J = 8.2$  Hz, 1H), 7.84 (t,  $J = 8.4$  Hz, 2H), 7.65 – 7.52 (m, 2H), 7.49 – 7.40 (m, 2H), 7.39 – 7.28 (m, 2H), 7.09 (s, 1H).  $^{13}\text{C}$  NMR (101 MHz,  $\text{CDCl}_3$ )  $\delta$  180.53, 148.61, 137.85, 135.22, 133.95, 132.72, 131.17, 130.86, 130.47, 129.52, 129.28, 129.05, 128.96, 128.03, 127.74, 127.33, 127.13, 123.76, 123.50. HRMS (ESI) calcd for  $[\text{C}_{19}\text{H}_{11}\text{ClSO} + \text{H}]^+$  323.0297, found 323.02967.

**4.1.1.4 2-(3-chlorophenyl)-4H-benzo[h]thiochromen-4-one (3d).** Pale white solid, yield: 52%;  $^1\text{H}$  NMR (400 MHz,  $\text{CDCl}_3$ )  $\delta$  8.44 (d,  $J = 8.8$  Hz, 1H), 8.33 (d,  $J = 7.9$  Hz, 1H), 7.91 – 7.79 (m, 2H), 7.68 (s, 1H), 7.66 – 7.53 (m, 3H), 7.49 – 7.35 (m, 2H), 7.25 (s, 1H).  $^{13}\text{C}$  NMR (101 MHz,  $\text{CDCl}_3$ )  $\delta$  180.81, 149.36, 138.34, 136.94, 135.35, 134.01, 130.73, 130.56, 129.52, 129.37, 129.07, 129.02, 128.16, 127.42, 127.23, 125.27, 124.52, 123.71, 123.52. HRMS (ESI) calcd for  $[\text{C}_{19}\text{H}_{11}\text{ClSO} + \text{H}]^+$  323.0297, found 323.02927.

**4.1.1.5 2-(4-chlorophenyl)-4H-benzo[h]thiochromen-4-one (3e).** Pale white solid, yield: 45%;  $^1\text{H}$  NMR (400 MHz,  $\text{CDCl}_3$ )  $\delta$  8.43 (d,  $J = 8.8$  Hz, 1H), 8.31 (d,  $J = 6.9$  Hz, 1H), 7.93 – 7.78 (m, 2H), 7.65 – 7.56 (m, 4H), 7.43 (d,  $J = 8.1$  Hz, 2H), 7.24 (s, 1H).  $^{13}\text{C}$  NMR (101 MHz,  $\text{CDCl}_3$ )  $\delta$  180.84, 149.70, 137.09, 136.93, 135.03, 134.00, 129.57, 129.46, 129.35, 129.04, 129.02, 128.32, 128.11, 127.39, 124.12, 123.70, 123.50. HRMS (ESI) calcd for  $[\text{C}_{19}\text{H}_{11}\text{ClSO} + \text{H}]^+$  323.0297, found 323.02919.

**4.1.2 General procedure for the preparation of 2-substituted phenyl-4H-benzo[h]thiochromen-4-one 1,1-dioxide derivatives 4a-b**

To a solution of thio naphthoflavone (**3**, 2 mmol) in acetic acid (4 ml) was added 1g of 30% aqueous hydrogen peroxide solution. The mixture was heated for 10 hours at 60 °C. After cooling, the reaction mixture was poured into an ice-water solution and then resulting solid was filtered and washed with water. Recrystallization from ethanol gave compounds **4a-b**.

**4.1.2.1 2-phenyl-4H-benzo[h]thiochromen-4-one 1,1-dioxide (4a).** yellow-green solid, yield: 78%;  $^1\text{H}$  NMR (400 MHz,  $\text{CDCl}_3$ )  $\delta$  8.87 (d,  $J = 7.9$  Hz, 1H), 8.15 (d,  $J = 8.7$  Hz, 1H), 8.05 (d,  $J = 8.6$  Hz, 1H), 7.96 – 7.81 (m, 3H), 7.76 – 7.61 (m, 2H), 7.58 – 7.41 (m, 3H), 6.82 (s, 1H).  $^{13}\text{C}$  NMR (101 MHz,  $\text{CDCl}_3$ )  $\delta$  178.59, 153.92, 138.06, 136.28, 133.52, 131.77, 129.86, 129.20, 129.11, 129.08, 128.72, 127.96, 127.13, 126.46, 126.11, 122.14. HRMS (ESI) calcd for  $[\text{C}_{19}\text{H}_{11}\text{ClSO} + \text{H}]^+$  323.0297, found 323.02919. HRMS (ESI) calcd for  $[\text{C}_{19}\text{H}_{12}\text{SO}_3 + \text{Na}]^+$  343.0405, found 343.04019.

**4.1.2.2 2-(3-chlorophenyl)-4H-benzo[h]thiochromen-4-one 1,1-dioxide (4b).** yellow-green solid, yield: 75%;  $^1\text{H}$  NMR (400 MHz,  $\text{CDCl}_3$ )  $\delta$  8.85 (d,  $J = 7.6$  Hz, 1H), 8.14 (d,  $J = 8.3$  Hz, 1H), 8.06 (d,  $J = 8.4$  Hz, 1H), 7.90 (d,  $J = 6.7$  Hz, 1H), 7.84 (s, 1H), 7.79 – 7.63 (m, 3H), 7.49 (d,  $J = 7.9$  Hz, 1H), 7.40 (t,  $J = 7.6$  Hz, 1H), 6.80 (s, 1H).  $^{13}\text{C}$  NMR (101 MHz,  $\text{CDCl}_3$ )  $\delta$  178.34, 152.52, 137.83, 136.31, 135.24, 133.67, 131.82, 130.45, 130.28, 130.00, 129.30, 129.12, 129.10, 128.63, 127.33, 127.03, 126.39, 126.05, 122.13. HRMS (ESI) calcd for  $[\text{C}_{19}\text{H}_{11}\text{ClSO}_3 + \text{Na}]^+$  377.0015, found 377.00095.

**4.1.3 General procedure for the preparation of 2-substituted phenyl-4H-benzo[h]chromen-4-one derivatives 9a-w**

The 1-(1-hydroxynaphthalen-2-yl)ethan-1-one (**6**) as a key intermediate was

obtained from commercially available naphthalen-1-ol (**5**) according to the literature procedure[18].

To a stirred solution of 1-(1-hydroxynaphthalen-2-yl)ethan-1-one **6** (2 mmol) in dry DMF (10 ml), benzoic acid derivative (2.2 mmol, commercially available or prepared according to the reported literature procedure), EDCI (3 mmol) and DMAP (3 mmol) were added and the resultant solution stirred for overnight at room temperature. After completion of the reaction as indicated by TLC, the reaction mixture was poured into an ice-water solution. the resulting mixture was extracted with EtOAc. The combined organic extracts were washed with saturated NaCl aqueous, dried over Na<sub>2</sub>SO<sub>4</sub>. the solvent was removed under vacuum and the crude residue was subjected to silica gel column chromatography to give intermediate **7**.

To a stirred solution of intermediate **7** (1mmol) in dry DMF (5 ml), NaH (10 mmol) was added and the resultant solution stirred for 5 hours at room temperature. After completion of the reaction as indicated by TLC, the reaction mixture was quenched with saturated ammonium chloride ice water solution and the precipitate obtained was filtered. After drying, this crude product **8** can be used directly without further purification.

Intermediate **8** (0.5 mmol) was dissolved in H<sub>2</sub>SO<sub>4</sub>-EtOH solution (10%, 25 ml). The resultant solution was kept for stirring at 90 °C till completion of the reaction (TLC monitoring). Solvents were removed under vacuum and the residue was purified by column chromatography using silica gel to give compounds **9a-w**.

**4.1.3.1 2-(2-fluorophenyl)-4H-benzo[h]chromen-4-one (9a).** Pale white solid, yield: 63%; <sup>1</sup>H NMR (400 MHz, CDCl<sub>3</sub>) δ 8.43 (d, *J* = 7.1 Hz, 1H), 8.06 (d, *J* = 8.6 Hz, 1H), 7.92 (t, *J* = 7.3 Hz, 1H), 7.82 (d, *J* = 7.1 Hz, 1H), 7.67 (d, *J* = 8.5 Hz, 1H), 7.63 – 7.52 (m, 2H), 7.46 (d, *J* = 5.7 Hz, 1H), 7.29 (t, *J* = 7.4 Hz, 1H), 7.17 (d, *J* = 9.9 Hz, 1H), 6.97 (s, 1H). <sup>13</sup>C NMR (101 MHz, CDCl<sub>3</sub>) δ 178.10, 160.46 (d, *J* = 254.0 Hz), 158.25 (d, *J* = 4.0 Hz), 153.66, 135.95, 132.90 (d, *J* = 9.0 Hz), 129.32, 128.94 (d, *J* = 2.0 Hz), 128.17, 127.19, 125.39, 124.78 (d, *J* = 3.0 Hz), 123.98, 122.32, 120.62, 120.33 (d, *J* = 10.0 Hz), 120.05, 117.12 (d, *J* = 22.0 Hz), 113.29 (d, *J* = 10.0 Hz). HRMS (ESI) calcd for [C<sub>19</sub>H<sub>11</sub>FO<sub>2</sub> + H]<sup>+</sup> 291.0821, found 291.08226; calcd for [C<sub>19</sub>H<sub>11</sub>FO<sub>2</sub> + Na]<sup>+</sup> 313.0641, found 313.06454.

**4.1.3.2 2-(3-fluorophenyl)-4H-benzo[h]chromen-4-one (9b).** Pale white solid, yield: 67%; <sup>1</sup>H NMR (400 MHz, CDCl<sub>3</sub>) δ 8.49 (d, *J* = 3.2 Hz, 1H), 8.08 (d, *J* = 8.7 Hz, 1H), 7.86 (d, *J* = 5.2 Hz, 1H), 7.71 (d, *J* = 8.3 Hz, 2H), 7.64 (d, *J* = 7.0 Hz, 3H), 7.48 (dd, *J* = 14.2, 7.1 Hz, 1H), 7.19 (d, *J* = 5.9 Hz, 1H), 6.87 (s, 1H). <sup>13</sup>C NMR (101 MHz, CDCl<sub>3</sub>) δ 178.03, 163.07 (d, *J* = 246.0 Hz), 161.15 (d, *J* = 3.0 Hz), 153.45, 136.04, 134.08 (d, *J* = 8.0 Hz), 130.91 (d, *J* = 8.0 Hz), 129.40, 128.28, 127.30, 125.58, 123.97, 122.25, 121.93 (d, *J* = 3.0 Hz), 120.64, 120.25, 118.48 (d, *J* = 21.0 Hz), 113.37 (d, *J* = 24.0 Hz), 109.34. HRMS (ESI) calcd for [C<sub>19</sub>H<sub>11</sub>FO<sub>2</sub> + H]<sup>+</sup> 291.0821, found 291.08264; calcd for [C<sub>19</sub>H<sub>11</sub>FO<sub>2</sub> + Na]<sup>+</sup> 313.0641, found 313.06429.

**4.1.3.3 2-(4-fluorophenyl)-4H-benzo[h]chromen-4-one (9c).** Pale white solid, yield: 68%; <sup>1</sup>H NMR (400 MHz, CDCl<sub>3</sub>) δ 8.45 (d, *J* = 6.9 Hz, 1H), 8.05 (d, *J* = 8.6 Hz, 1H), 8.00 – 7.87 (m, 2H), 7.83 (d, *J* = 5.4 Hz, 1H), 7.67 (d, *J* = 8.7 Hz, 1H), 7.61 (d, *J* = 6.8 Hz, 2H), 7.18 (t, *J* = 8.1 Hz, 2H), 6.81 (s, 1H). <sup>13</sup>C NMR (101 MHz, CDCl<sub>3</sub>) δ 178.02,



164.68 (d,  $J = 252.0$  Hz), 161.64, 153.39, 135.98, 129.29, 128.41, 128.32, 128.25, 128.07(d,  $J = 3.0$  Hz), 127.20, 125.43, 123.95, 122.18, 120.65, 120.08, 116.54, 116.32, 108.49. HRMS (ESI) calcd for  $[\text{C}_{19}\text{H}_{11}\text{FO}_2 + \text{H}]^+$  291.0821, found 291.08240; calcd for  $[\text{C}_{19}\text{H}_{11}\text{FO}_2 + \text{Na}]^+$  313.0641, found 313.06420.

**4.1.3.4 2-(2-chlorophenyl)-4H-benzo[h]chromen-4-one (9d).** Pale white solid, yield: 63%;  $^1\text{H}$  NMR (400 MHz,  $\text{CDCl}_3$ )  $\delta$  8.46 (d,  $J = 8.0$  Hz, 1H), 8.11 (d,  $J = 8.7$  Hz, 1H), 7.85 (d,  $J = 7.8$  Hz, 1H), 7.72 (d,  $J = 8.6$  Hz, 1H), 7.68 – 7.54 (m, 3H), 7.51 (d,  $J = 7.7$  Hz, 1H), 7.45 – 7.33 (m, 2H), 6.75 (s, 1H).  $^{13}\text{C}$  NMR (101 MHz,  $\text{CDCl}_3$ )  $\delta$  177.99, 162.02, 154.04, 135.97, 132.93, 131.88, 131.82, 130.99, 130.90, 129.39, 128.10, 127.27, 127.22, 125.47, 124.09, 122.51, 120.64, 120.09, 114.06. HRMS (ESI) calcd for  $[\text{C}_{19}\text{H}_{11}\text{ClO}_2 + \text{H}]^+$  307.0526, found 307.05328; calcd for  $[\text{C}_{19}\text{H}_{11}\text{ClO}_2 + \text{Na}]^+$  329.0345, found 329.03510.

**4.1.3.5 2-(3-chlorophenyl)-4H-benzo[h]chromen-4-one (9e).** Pale white solid, yield: 58%;  $^1\text{H}$  NMR (400 MHz,  $\text{DMSO}-d_6$ )  $\delta$  8.71 – 8.58 (m, 1H), 8.29 – 8.17 (m, 2H), 8.14 – 8.05 (m, 1H), 7.98 (d,  $J = 8.6$  Hz, 1H), 7.92 (d,  $J = 8.8$  Hz, 1H), 7.82 (dd,  $J = 6.0, 3.1$  Hz, 2H), 7.74 – 7.61 (m, 2H), 7.28 (s, 1H).  $^{13}\text{C}$  NMR (101 MHz,  $\text{DMSO}-d_6$ )  $\delta$  177.23, 160.78, 153.20, 135.90, 134.55, 133.78, 131.89, 131.53, 130.09, 128.68, 128.21, 126.42, 125.99, 125.52, 123.83, 122.77, 120.33, 120.07, 109.47. HRMS (ESI) calcd for  $[\text{C}_{19}\text{H}_{11}\text{ClO}_2 + \text{H}]^+$  307.0526, found 307.05352; calcd for  $[\text{C}_{19}\text{H}_{11}\text{ClO}_2 + \text{Na}]^+$  329.0345, found 329.03540.

**4.1.3.6 2-(4-chlorophenyl)-4H-benzo[h]chromen-4-one (9f).** Pale white solid, yield: 59%;  $^1\text{H}$  NMR (400 MHz,  $\text{CDCl}_3$ )  $\delta$  8.46 (s, 1H), 8.06 (d,  $J = 7.0$  Hz, 1H), 7.96 – 7.77 (m, 3H), 7.77 – 7.56 (m, 3H), 7.46 (d,  $J = 6.8$  Hz, 2H), 6.85 (s, 1H).  $^{13}\text{C}$  NMR (101 MHz,  $\text{CDCl}_3$ )  $\delta$  177.97, 161.52, 153.44, 137.85, 136.03, 130.34, 129.50, 129.35, 128.28, 127.43, 127.24, 125.52, 123.97, 122.19, 120.65, 120.17, 108.83. HRMS (ESI) calcd for  $[\text{C}_{19}\text{H}_{11}\text{ClO}_2 + \text{H}]^+$  307.0526, found 307.05344; calcd for  $[\text{C}_{19}\text{H}_{11}\text{ClO}_2 + \text{Na}]^+$  329.0345, found 329.03518.

**4.1.3.7 2-(3-methoxyphenyl)-4H-benzo[h]chromen-4-one (9g).** Pale white solid, yield: 75%;  $^1\text{H}$  NMR (400 MHz,  $\text{CDCl}_3$ )  $\delta$  8.42 (s, 1H), 8.03 (d,  $J = 7.2$  Hz, 1H), 7.79 (s, 1H), 7.64 (d,  $J = 8.0$  Hz, 1H), 7.58 (s, 2H), 7.46 (d,  $J = 6.5$  Hz, 1H), 7.37 (d,  $J = 7.4$  Hz, 2H), 6.98 (d,  $J = 6.8$  Hz, 1H), 6.82 (s, 1H), 3.81 (s, 3H).  $^{13}\text{C}$  NMR (101 MHz,  $\text{CDCl}_3$ )  $\delta$  178.15, 162.30, 160.00, 153.40, 135.92, 133.14, 130.23, 129.20, 128.15, 127.13, 125.29, 124.01, 122.25, 120.64, 120.18, 118.55, 116.76, 111.85, 108.89, 55.44. HRMS (ESI) calcd for  $[\text{C}_{20}\text{H}_{14}\text{O}_3 + \text{H}]^+$  303.1021, found 303.10284; calcd for  $[\text{C}_{20}\text{H}_{14}\text{O}_3 + \text{Na}]^+$  325.0841, found 325.08477.

**4.1.3.8 2-(4-methoxyphenyl)-4H-benzo[h]chromen-4-one (9h).** Pale white solid, yield: 72%;  $^1\text{H}$  NMR (400 MHz,  $\text{CDCl}_3$ )  $\delta$  8.44 (s, 1H), 8.12 – 7.97 (m, 1H), 7.93 – 7.75 (m, 3H), 7.71 – 7.46 (m, 3H), 6.95 (s, 2H), 6.77 (d,  $J = 5.1$  Hz, 1H), 3.80 (s, 3H).  $^{13}\text{C}$  NMR (101 MHz,  $\text{CDCl}_3$ )  $\delta$  178.12, 162.30, 153.35, 135.90, 129.09, 128.17, 127.84, 126.94, 125.12, 124.07, 122.24, 120.71, 120.06, 114.55, 107.25, 55.45. HRMS (ESI) calcd for  $[\text{C}_{20}\text{H}_{14}\text{O}_3 + \text{H}]^+$  303.1021, found 303.10316; calcd for  $[\text{C}_{20}\text{H}_{14}\text{O}_3 + \text{Na}]^+$  325.0841, found 325.08477.

**4.1.3.9 2-(3-hydroxyphenyl)-4H-benzo[h]chromen-4-one (9i).** Pale white solid, yield:

54%;  $^1\text{H}$  NMR (400 MHz, DMSO- $d_6$ )  $\delta$  9.91 (s, 1H), 8.59 (d,  $J$  = 4.9 Hz, 1H), 8.14 – 8.04 (m, 1H), 7.97 (d,  $J$  = 8.6 Hz, 1H), 7.90 (d,  $J$  = 8.4 Hz, 1H), 7.80 (d,  $J$  = 4.8 Hz, 2H), 7.67 – 7.56 (m, 8.8 Hz, 2H), 7.40 (t,  $J$  = 7.7 Hz, 1H), 7.05 (s, 1H), 7.01 (d,  $J$  = 7.8 Hz, 1H).  $^{13}\text{C}$  NMR (101 MHz, DMSO- $d_6$ )  $\delta$  177.26, 162.41, 158.44, 153.14, 135.91, 132.89, 130.85, 130.01, 128.77, 128.16, 125.81, 123.94, 122.48, 120.46, 120.09, 119.23, 117.60, 113.19, 108.50. HRMS (ESI) calcd for  $[\text{C}_{19}\text{H}_{12}\text{O}_3 + \text{H}]^+$  289.0865, found 289.08708.

4.1.3.10 2-(3-(trifluoromethyl)phenyl)-4H-benzo[h]chromen-4-one (**9j**). Pale white solid, yield: 52%;  $^1\text{H}$  NMR (400 MHz,  $\text{CDCl}_3$ )  $\delta$  8.44 (d,  $J$  = 3.4 Hz, 1H), 8.16 (s, 1H), 8.12 – 8.01 (m, 2H), 7.91 – 7.81 (m, 1H), 7.75 (d,  $J$  = 7.6 Hz, 1H), 7.69 (d,  $J$  = 8.9 Hz, 1H), 7.67 – 7.59 (m, 3H), 6.89 (s, 1H).  $^{13}\text{C}$  NMR (101 MHz,  $\text{CDCl}_3$ )  $\delta$  177.81, 160.88, 153.47, 136.09, 132.89, 132.02, 131.69, 129.86, 129.43, 129.31, 128.30, 127.98 (d,  $J$  = 4.0 Hz), 127.38, 125.67, 123.94, 122.98 (q,  $J$  = 4.0 Hz), 122.13, 120.62, 120.28, 109.60. HRMS (ESI) calcd for  $[\text{C}_{20}\text{H}_{11}\text{F}_3\text{O}_2 + \text{H}]^+$  341.0789, found 341.07987.

4.1.3.11 2-(3-(dimethylamino)phenyl)-4H-benzo[h]chromen-4-one (**9k**). Pale white solid, yield: 54%;  $^1\text{H}$  NMR (400 MHz,  $\text{CDCl}_3$ )  $\delta$  8.57 (s, 1H), 8.16 (d,  $J$  = 8.6 Hz, 1H), 7.91 (s, 1H), 7.76 (d,  $J$  = 8.5 Hz, 1H), 7.69 (s, 2H), 7.45 – 7.31 (m, 2H), 7.25 – 7.19 (m, 1H), 7.01 – 6.85 (m, 2H), 3.06 (s, 6H).  $^{13}\text{C}$  NMR (101 MHz,  $\text{CDCl}_3$ )  $\delta$  178.41, 163.65, 153.56, 150.61, 135.96, 132.69, 129.83, 129.15, 128.21, 127.12, 125.22, 124.19, 122.33, 120.75, 120.25, 115.55, 114.56, 109.70, 108.78, 40.60.

4.1.3.12 2-(3,5-dichlorophenyl)-4H-benzo[h]chromen-4-one (**9l**). Pale white solid, yield: 60%;  $^1\text{H}$  NMR (400 MHz,  $\text{CDCl}_3$ )  $\delta$  8.47 (d,  $J$  = 5.2 Hz, 1H), 8.08 (d,  $J$  = 8.6 Hz, 1H), 7.89 (d,  $J$  = 6.7 Hz, 1H), 7.79 (s, 2H), 7.73 (d,  $J$  = 8.5 Hz, 1H), 7.70 – 7.65 (m, 2H), 7.49 (s, 1H), 6.84 (s, 1H).  $^{13}\text{C}$  NMR (101 MHz,  $\text{CDCl}_3$ )  $\delta$  177.66, 159.72, 153.47, 136.14, 136.11, 134.95, 131.20, 129.52, 128.33, 127.44, 125.80, 124.60, 123.90, 122.20, 120.61, 120.35, 110.02. HRMS (ESI) calcd for  $[\text{C}_{19}\text{H}_{10}\text{Cl}_2\text{O}_2 + \text{H}]^+$  341.0136, found 341.01366.

4.1.3.13 2-(3,4-difluorophenyl)-4H-benzo[h]chromen-4-one (**9m**). Pale white solid, yield: 47%;  $^1\text{H}$  NMR (400 MHz, DMSO- $d_6$ )  $\delta$  8.74 (d,  $J$  = 8.3 Hz, 1H), 8.42 – 8.31 (m, 1H), 8.21 – 8.09 (m, 2H), 7.98 (q,  $J$  = 8.6 Hz, 2H), 7.86 – 7.80 (m, 2H), 7.70 (dd,  $J$  = 18.3, 8.8 Hz, 1H), 7.29 (s, 1H).  $^{13}\text{C}$  NMR (101 MHz,  $\text{CDCl}_3$ )  $\delta$  177.9, 160.4, 153.4, 152.34 (dd,  $J$  = 254.0 Hz,  $J$  = 13.0 Hz), 150.75 (dd,  $J$  = 250.0 Hz,  $J$  = 13.0 Hz), 136.09, 129.46, 129.03, 128.34, 127.36, 125.69, 123.90, 122.82 (dd,  $J$  = 7.0 Hz,  $J$  = 4.0 Hz), 122.16, 120.63, 120.16, 118.37 (d,  $J$  = 18.0 Hz), 115.56 (d,  $J$  = 20.0 Hz), 109.12. HRMS (ESI) calcd for  $[\text{C}_{19}\text{H}_{10}\text{F}_2\text{O}_2 + \text{H}]^+$  309.0727, found 309.07285.

4.1.3.14 2-(3,4,5-trimethoxyphenyl)-4H-benzo[h]chromen-4-one (**9n**). Pale white solid, yield: 58%;  $^1\text{H}$  NMR (400 MHz,  $\text{CDCl}_3$ )  $\delta$  8.38 (d,  $J$  = 6.9 Hz, 1H), 8.03 (d,  $J$  = 8.7 Hz, 1H), 7.82 (d,  $J$  = 5.5 Hz, 1H), 7.65 (d,  $J$  = 9.1 Hz, 1H), 7.62 – 7.54 (m, 2H), 7.09 (s, 2H), 6.78 (s, 1H), 3.91 (s, 6H), 3.88 (s, 3H).  $^{13}\text{C}$  NMR (101 MHz,  $\text{CDCl}_3$ )  $\delta$  177.99, 162.41, 153.60, 153.32, 141.10, 135.95, 129.17, 128.28, 127.18, 127.02, 125.31, 123.96, 121.94, 120.64, 120.10, 108.43, 103.60, 61.04, 56.32. HRMS (ESI) calcd for  $[\text{C}_{22}\text{H}_{18}\text{O}_5 + \text{H}]^+$  363.1232, found 363.12361.

4.1.3.15 2-(3-chloro-5-methoxyphenyl)-4H-benzo[h]chromen-4-one (**9o**). Pale white solid, yield: 61%;  $^1\text{H}$  NMR (400 MHz,  $\text{CDCl}_3$ )  $\delta$  8.57 – 8.44 (m, 1H), 8.09 (d,  $J$  = 8.6 Hz, 1H), 7.87 (s, 1H), 7.72 (d,  $J$  = 9.2 Hz, 1H), 7.68 – 7.59 (m, 2H), 7.51 (s, 1H), 7.33 (s,

1H), 7.01 (s, 1H), 6.84 (s, 1H), 3.85 (s, 3H).  $^{13}\text{C}$  NMR (101 MHz,  $\text{CDCl}_3$ )  $\delta$  177.02, 160.14, 159.73, 152.53, 135.09, 135.03, 133.41, 128.42, 127.29, 126.34, 124.61, 123.01, 121.30, 119.66, 119.30, 117.65, 115.81, 109.84, 108.57, 54.82. HRMS (ESI) calcd for  $[\text{C}_{20}\text{H}_{13}\text{ClO}_3 + \text{H}]^+$  337.0631, found 337.06357.

**4.1.3.16 2-(naphthalen-2-yl)-4H-benzo[h]chromen-4-one (9p).** Pale white solid, yield: 61%;  $^1\text{H}$  NMR (400 MHz,  $\text{CDCl}_3$ )  $\delta$  8.45 (d,  $J = 6.8$  Hz, 1H), 8.31 (s, 1H), 8.02 (d,  $J = 8.6$  Hz, 1H), 7.91 – 7.68 (m, 5H), 7.67 – 7.52 (m, 3H), 7.46 (d,  $J = 4.1$  Hz, 2H), 6.90 (s, 1H).  $^{13}\text{C}$  NMR (101 MHz,  $\text{CDCl}_3$ )  $\delta$  178.07, 162.36, 153.40, 135.92, 134.50, 132.80, 129.21, 129.01, 128.99, 128.85, 128.19, 127.97, 127.78, 127.13, 127.07, 126.61, 125.28, 124.01, 122.31, 122.28, 120.66, 120.17, 108.88. HRMS (ESI) calcd for  $[\text{C}_{23}\text{H}_{14}\text{O}_2 + \text{H}]^+$  323.1072, found 323.10747.

**4.1.3.17 2-(4-(4-methylpiperazin-1-yl)phenyl)-4H-benzo[h]chromen-4-one (9q).** Pale yellow solid, yield: 69%;  $^1\text{H}$  NMR (400 MHz,  $\text{DMSO}-d_6$ )  $\delta$  8.69 – 8.59 (m, 1H), 8.16 – 8.05 (m, 3H), 7.97 (d,  $J = 8.6$  Hz, 1H), 7.90 (d,  $J = 8.8$  Hz, 1H), 7.83 – 7.76 (m, 2H), 7.17 (d,  $J = 8.7$  Hz, 2H), 7.06 (s, 1H), 4.06 (brs, 2H), 3.46 (brs, 2H), 3.30 – 3.20 (brs, 2H), 3.15 (brs, 2H), 2.80 (s, 3H).  $^{13}\text{C}$  NMR (101 MHz,  $\text{DMSO}-d_6$ )  $\delta$  177.06, 162.72, 153.00, 152.13, 135.82, 129.88, 128.74, 128.20, 128.12, 125.61, 123.94, 122.63, 121.57, 120.53, 120.04, 115.49, 106.36, 52.16, 44.64, 42.36. HRMS (ESI) calcd for  $[\text{C}_{24}\text{H}_{22}\text{N}_2\text{O}_2 + \text{H}]^+$  371.1760, found 371.17762.

**4.1.3.18 2-(3-(4-methylpiperazin-1-yl)phenyl)-4H-benzo[h]chromen-4-one (9r).** Pale white solid, yield: 66%;  $^1\text{H}$  NMR (400 MHz,  $\text{CDCl}_3$ )  $\delta$  8.48 – 8.38 (m, 1H), 8.05 (d,  $J = 8.6$  Hz, 1H), 7.87 – 7.73 (m, 1H), 7.65 (d,  $J = 8.7$  Hz, 1H), 7.62 – 7.55 (m, 2H), 7.42 – 7.30 (m, 3H), 7.02 (d,  $J = 7.8$  Hz, 1H), 6.82 (s, 1H), 3.32 – 3.18 (m, 4H), 2.59 – 2.50 (m, 4H), 2.31 (s, 3H).  $^{13}\text{C}$  NMR (101 MHz,  $\text{CDCl}_3$ )  $\delta$  178.24, 163.20, 153.47, 151.75, 135.93, 132.78, 129.88, 129.17, 128.19, 127.12, 125.25, 124.09, 122.25, 120.70, 120.22, 119.15, 117.44, 113.20, 108.84, 54.94, 48.84, 46.12. HRMS (ESI) calcd for  $[\text{C}_{24}\text{H}_{22}\text{N}_2\text{O}_2 + \text{H}]^+$  371.1760, found 371.17770.

**4.1.3.19 2-(3-chloro-5-(4-methylpiperazin-1-yl)phenyl)-4H-benzo[h]chromen-4-one (9s).** Pale white solid, yield: 64%;  $^1\text{H}$  NMR (400 MHz,  $\text{CDCl}_3$ )  $\delta$  8.55 – 8.44 (m, 1H), 8.09 (d,  $J = 8.7$  Hz, 1H), 7.91 – 7.84 (m, 1H), 7.73 (d,  $J = 8.7$  Hz, 1H), 7.69 – 7.62 (m, 2H), 7.38 (s, 1H), 7.25 (s, 1H), 6.99 (s, 1H), 6.84 (s, 1H), 3.33 – 3.20 (m, 4H), 2.64 – 2.52 (m, 4H), 2.33 (s, 3H).  $^{13}\text{C}$  NMR (101 MHz,  $\text{CDCl}_3$ )  $\delta$  178.09, 162.00, 153.54, 152.51, 136.05, 136.00, 134.16, 129.35, 128.29, 127.31, 125.52, 124.05, 122.28, 120.68, 120.30, 118.32, 116.82, 111.34, 109.45, 54.72, 48.37, 46.04. HRMS (ESI) calcd for  $[\text{C}_{24}\text{H}_{21}\text{ClN}_2\text{O}_2 + \text{H}]^+$  405.1370, found 405.13835.

**4.1.3.20 2-(3-morpholinophenyl)-4H-benzo[h]chromen-4-one (9t).** Pale white solid, yield: 69%;  $^1\text{H}$  NMR (400 MHz,  $\text{CDCl}_3$ )  $\delta$  8.52 – 8.40 (m, 1H), 8.07 (d,  $J = 8.5$  Hz, 1H), 7.88 – 7.79 (m, 1H), 7.68 (d,  $J = 8.6$  Hz, 1H), 7.64 – 7.57 (m, 2H), 7.45 (d,  $J = 7.4$  Hz, 1H), 7.42 – 7.32 (m, 2H), 7.04 (d,  $J = 7.7$  Hz, 1H), 6.84 (s, 1H), 3.92 – 3.79 (m, 4H), 3.27 – 3.12 (m, 4H).  $^{13}\text{C}$  NMR (101 MHz,  $\text{CDCl}_3$ )  $\delta$  178.21, 163.04, 153.50, 151.63, 135.97, 132.93, 130.01, 129.22, 128.24, 127.18, 125.32, 124.10, 122.26, 120.72, 120.25, 118.86, 117.99, 113.02, 108.97, 66.73, 49.16. HRMS (ESI) calcd for  $[\text{C}_{23}\text{H}_{19}\text{NO}_3 + \text{H}]^+$  358.1443, found 358.14512.



**4.1.3.21 2-(pyridin-2-yl)-4H-benzo[h]chromen-4-one (9u).** Pale white solid, yield: 43%;  $^1\text{H}$  NMR (400 MHz,  $\text{CDCl}_3$ )  $\delta$  8.70 (d,  $J = 4.2$  Hz, 1H), 8.57 – 8.47 (m, 1H), 8.15 (d,  $J = 7.8$  Hz, 1H), 8.10 (d,  $J = 8.7$  Hz, 1H), 7.92 – 7.81 (m, 2H), 7.70 (d,  $J = 8.7$  Hz, 1H), 7.63 (dd,  $J = 6.2, 3.2$  Hz, 2H), 7.49 (s, 1H), 7.39 (dd,  $J = 7.1, 4.8$  Hz, 1H).  $^{13}\text{C}$  NMR (101 MHz,  $\text{CDCl}_3$ )  $\delta$  178.31, 160.79, 153.33, 150.16, 149.56, 148.07, 137.21, 136.03, 129.29, 128.27, 127.18, 125.57, 125.47, 124.05, 122.27, 120.88, 120.85, 110.09. HRMS (ESI) calcd for  $[\text{C}_{18}\text{H}_{11}\text{NO}_2 + \text{H}]^+$  274.0868, found 274.08778.

**4.1.3.22 2-(pyridin-3-yl)-4H-benzo[h]chromen-4-one (9v).** Pale white solid, yield: 55%;  $^1\text{H}$  NMR (400 MHz,  $\text{CDCl}_3$ )  $\delta$  9.19 (s, 1H), 8.72 (s, 1H), 8.42 (s, 1H), 8.16 (s, 1H), 8.03 (d,  $J = 7.9$  Hz, 1H), 7.82 (s, 1H), 7.67 (d,  $J = 8.3$  Hz, 1H), 7.61 (s, 2H), 7.45 (s, 1H), 6.86 (s, 1H).  $^{13}\text{C}$  NMR (101 MHz,  $\text{CDCl}_3$ )  $\delta$  177.60, 160.15, 153.44, 152.09, 147.37, 136.01, 133.39, 129.43, 128.25, 127.96, 127.32, 125.64, 123.86, 123.81, 122.12, 120.57, 120.27, 109.59. HRMS (ESI) calcd for  $[\text{C}_{18}\text{H}_{11}\text{NO}_2 + \text{H}]^+$  274.0868, found 274.08748.

**4.1.3.23 2-(pyridin-4-yl)-4H-benzo[h]chromen-4-one (9w).** Pale white solid, yield: 59%;  $^1\text{H}$  NMR (400 MHz,  $\text{CDCl}_3$ )  $\delta$  8.81 (d,  $J = 4.7$  Hz, 2H), 8.59 – 8.46 (m, 1H), 8.10 (d,  $J = 8.7$  Hz, 1H), 7.97 – 7.88 (m, 1H), 7.82 (d,  $J = 4.8$  Hz, 2H), 7.75 (d,  $J = 8.8$  Hz, 1H), 7.71 – 7.64 (m, 2H), 6.99 (s, 1H).  $^{13}\text{C}$  NMR (101 MHz,  $\text{CDCl}_3$ )  $\delta$  177.69, 159.79, 153.47, 150.94, 139.38, 136.19, 129.60, 128.38, 127.44, 125.89, 123.97, 122.19, 120.61, 120.54, 119.74, 110.60. HRMS (ESI) calcd for  $[\text{C}_{18}\text{H}_{11}\text{NO}_2 + \text{H}]^+$  274.0868, found 274.08763.

**4.1.4 General procedure for the preparation of 2-substituted phenyl-4H-benzo[h]chromen-4-thione derivatives 10a-h**

To a solution of compound **9** (1 equivalent) in dry toluene (20 ml), Lawesson's reagent (2 equivalents) was added and the resultant solution was kept for stirring at 110 °C till completion of the reaction (TLC monitoring). Solvents were removed under vacuum and the residue was purified by column chromatography using silica gel to give compounds **10a-h**.

**4.1.4.1 2-phenyl-4H-benzo[h]chromene-4-thione (10a).** Pale yellow solid, yield: 82%;  $^1\text{H}$  NMR (400 MHz,  $\text{DMSO}-d_6$ )  $\delta$  8.78 (s, 1H), 8.46 (d,  $J = 7.9$  Hz, 1H), 8.35 (d,  $J = 6.7$  Hz, 2H), 8.11 (d,  $J = 10.3$  Hz, 2H), 8.00 (d,  $J = 8.4$  Hz, 1H), 7.87 (s, 2H), 7.67 (d,  $J = 6.3$  Hz, 3H).  $^{13}\text{C}$  NMR (101 MHz,  $\text{DMSO}-d_6$ )  $\delta$  200.16, 153.99, 148.47, 135.97, 132.53, 130.86, 130.52, 129.86, 128.67, 128.46, 127.23, 126.87, 126.53, 123.90, 123.55, 123.43, 120.78. HRMS (ESI) calcd for  $[\text{C}_{19}\text{H}_{12}\text{OS} + \text{H}]^+$  289.0687, found 289.06936.

**4.1.4.2 2-(2-fluorophenyl)-4H-benzo[h]chromene-4-thione (10b).** Pale yellow solid, yield: 74%;  $^1\text{H}$  NMR (400 MHz,  $\text{CDCl}_3$ )  $\delta$  8.48 (d,  $J = 8.7$  Hz, 2H), 8.02 – 7.94 (m, 1H), 7.89 (s, 1H), 7.82 (d,  $J = 7.8$  Hz, 1H), 7.68 (d,  $J = 8.9$  Hz, 1H), 7.62 (t,  $J = 7.2$  Hz, 2H), 7.52 – 7.42 (m, 1H), 7.31 (t,  $J = 7.5$  Hz, 1H), 7.20 – 7.15 (m, 1H).  $^{13}\text{C}$  NMR (101 MHz,  $\text{CDCl}_3$ )  $\delta$  201.18, 160.54 (d,  $J = 256.0$  Hz), 149.67 (d,  $J = 5.0$  Hz), 148.65, 136.07, 133.09 (d,  $J = 9.0$  Hz), 129.69, 129.08, 128.18, 127.46, 126.97, 126.33, 125.17 (d,  $J = 11.0$  Hz), 124.95 (d,  $J = 4.0$  Hz), 123.96 (d,  $J = 18.0$  Hz), 123.07, 119.86 (d,  $J = 10.0$  Hz), 117.25 (d,  $J = 22.0$  Hz), 109.99. HRMS (ESI) calcd for  $[\text{C}_{19}\text{H}_{11}\text{FOS} + \text{H}]^+$  307.0593, found 307.05965.

**4.1.4.3 2-(3-fluorophenyl)-4H-benzo[h]chromene-4-thione (10c).** Pale yellow solid,

yield: 73%;  $^1\text{H}$  NMR (400 MHz,  $\text{CDCl}_3$ )  $\delta$  8.57 – 8.45 (m, 2H), 7.84 (d,  $J = 5.7$  Hz, 1H), 7.76 (d,  $J = 12.0$  Hz, 2H), 7.72 – 7.60 (m, 4H), 7.53 – 7.44 (m, 1H), 7.23 (d,  $J = 8.2$  Hz, 1H).  $^{13}\text{C}$  NMR (101 MHz,  $\text{CDCl}_3$ )  $\delta$  200.98, 163.17 (d,  $J = 246.0$  Hz), 152.01 (d,  $J = 2.0$  Hz), 148.42, 136.15, 133.55 (d,  $J = 8.0$  Hz), 131.04 (d,  $J = 8.0$  Hz), 129.77, 128.28, 127.56, 127.07, 126.47, 124.01, 123.86, 122.95, 122.08 (d,  $J = 3.0$  Hz), 121.64, 118.64 (d,  $J = 21.0$  Hz), 113.38 (d,  $J = 24.0$  Hz). HRMS (ESI) calcd for  $[\text{C}_{19}\text{H}_{11}\text{FOS} + \text{H}]^+$  307.0593, found 307.05952.

4.1.4.4 2-(3-chlorophenyl)-4H-benzo[h]chromene-4-thione (**10d**). Pale yellow solid, yield: 78%;  $^1\text{H}$  NMR (400 MHz,  $\text{DMSO}-d_6$ )  $\delta$  8.78 – 8.70 (m, 1H), 8.43 (d,  $J = 9.0$  Hz, 1H), 8.35 (s, 1H), 8.31 (d,  $J = 7.8$  Hz, 1H), 8.17 – 8.08 (m, 2H), 7.99 (d,  $J = 8.9$  Hz, 1H), 7.92 – 7.81 (m, 2H), 7.74 (d,  $J = 8.1$  Hz, 1H), 7.68 (t,  $J = 7.9$  Hz, 1H).  $^{13}\text{C}$  NMR (101 MHz,  $\text{DMSO}-d_6$ )  $\delta$  200.53, 152.60, 148.58, 136.07, 134.75, 133.22, 132.21, 131.71, 130.69, 128.74, 128.61, 127.12, 126.81, 126.78, 126.02, 123.92, 123.73, 123.38, 121.48. HRMS (ESI) calcd for  $[\text{C}_{19}\text{H}_{11}\text{ClOS} + \text{H}]^+$  323.0297, found 323.03025.

4.1.4.5 2-(3-methoxyphenyl)-4H-benzo[h]chromene-4-thione (**10e**). Pale yellow solid, yield: 80%;  $^1\text{H}$  NMR (400 MHz,  $\text{CDCl}_3$ )  $\delta$  8.59 – 8.23 (m, 2H), 7.84 – 7.65 (m, 2H), 7.65 – 7.43 (m, 4H), 7.41 – 7.22 (m, 2H), 7.07 – 6.93 (m, 1H), 3.80 (s, 3H).  $^{13}\text{C}$  NMR (101 MHz,  $\text{CDCl}_3$ )  $\delta$  200.63, 160.09, 153.21, 148.35, 135.98, 132.40, 130.35, 129.58, 128.13, 127.39, 126.84, 126.18, 123.98, 123.85, 122.91, 121.32, 118.79, 117.25, 111.69, 55.51. HRMS (ESI) calcd for  $[\text{C}_{20}\text{H}_{14}\text{O}_2\text{S} + \text{H}]^+$  319.0793, found 319.08003.

4.1.4.6 2-(4-fluorophenyl)-4H-benzo[h]chromene-4-thione (**10f**). Pale yellow solid, yield: 75%;  $^1\text{H}$  NMR (400 MHz,  $\text{CDCl}_3$ )  $\delta$  8.46 (d,  $J = 8.7$  Hz, 2H), 8.02 – 7.91 (m, 2H), 7.81 (d,  $J = 6.1$  Hz, 1H), 7.73 (s, 1H), 7.70 – 7.55 (m, 3H), 7.23 – 7.17 (m, 2H).  $^{13}\text{C}$  NMR (101 MHz,  $\text{CDCl}_3$ )  $\delta$  200.73, 163.17 (d,  $J = 253.0$  Hz), 152.57, 148.36, 136.07, 129.65, 128.63, 128.54, 128.25, 127.56, 127.45, 126.77, 126.29, 123.98, 123.91, 122.86, 121.02, 116.76, 116.54. HRMS (ESI) calcd for  $[\text{C}_{19}\text{H}_{11}\text{FOS} + \text{H}]^+$  307.0593, found 307.05930.

4.1.4.7 2-(4-chlorophenyl)-4H-benzo[h]chromene-4-thione (**10g**). Pale yellow solid, yield: 64%;  $^1\text{H}$  NMR (400 MHz,  $\text{CDCl}_3$ )  $\delta$  8.54 (t,  $J = 7.9$  Hz, 2H), 7.96 (d,  $J = 8.1$  Hz, 2H), 7.88 (d,  $J = 7.0$  Hz, 1H), 7.82 (s, 1H), 7.73 (d,  $J = 9.0$  Hz, 1H), 7.71 – 7.64 (m, 2H), 7.50 (d,  $J = 8.4$  Hz, 2H).  $^{13}\text{C}$  NMR (101 MHz,  $\text{CDCl}_3$ )  $\delta$  201.39, 152.82, 148.44, 138.07, 136.15, 129.79, 129.74, 129.70, 128.32, 127.62, 127.53, 126.97, 126.44, 124.04, 123.92, 122.93, 121.31. HRMS (ESI) calcd for  $[\text{C}_{19}\text{H}_{11}\text{ClOS} + \text{H}]^+$  323.0297, found 323.02968.

4.1.4.8 2-(3,4,5-trimethoxyphenyl)-4H-benzo[h]chromene-4-thione (**10h**). Pale yellow solid, yield: 77%;  $^1\text{H}$  NMR (400 MHz,  $\text{CDCl}_3$ )  $\delta$  8.48 (dd,  $J = 16.2, 8.1$  Hz, 2H), 7.85 (d,  $J = 6.7$  Hz, 1H), 7.76 (s, 1H), 7.71 – 7.61 (m, 3H), 7.18 (s, 2H), 3.94 (s, 6H), 3.90 (s, 3H).  $^{13}\text{C}$  NMR (101 MHz,  $\text{CDCl}_3$ )  $\delta$  200.39, 153.78, 153.56, 148.43, 141.49, 136.12, 129.59, 128.34, 127.49, 126.75, 126.29, 126.25, 124.01, 122.66, 121.11, 103.87, 61.07, 56.44. HRMS (ESI) calcd for  $[\text{C}_{22}\text{H}_{18}\text{O}_4\text{S} + \text{H}]^+$  379.1004, found 379.10178.

4.1.5 General procedure for the preparation of 2-substituted phenyl-4H-benzo[h]chromen-4-thione derivatives **11a-c**

To a solution of compound **10** (1 equivalent) in dry pyridine (20 ml), hydroxylamine hydrochloride (2 equivalents) was added and the resultant solution was kept for stirring

at 120 °C till completion of the reaction (TLC monitoring). Solvents were removed under vacuum and the residue was purified by column chromatography using silica gel to give compounds **11a-c**.

**4.1.5.1 (E)-2-phenyl-4H-benzo[h]chromen-4-one oxime (11a).** Pale white solid, yield: 78%; <sup>1</sup>H NMR (400 MHz, DMSO-*d*<sub>6</sub>) δ 11.05 (s, 1H), 8.48 (d, *J* = 7.7 Hz, 1H), 8.11 (d, *J* = 6.8 Hz, 2H), 8.03 (d, *J* = 7.7 Hz, 1H), 7.94 (d, *J* = 8.5 Hz, 1H), 7.82 (d, *J* = 8.7 Hz, 1H), 7.77 – 7.65 (m, 2H), 7.64 – 7.53 (m, 3H), 7.27 (s, 1H). <sup>13</sup>C NMR (101 MHz, DMSO-*d*<sub>6</sub>) δ 153.75, 146.77, 142.88, 134.28, 132.62, 130.94, 129.53, 128.45, 128.12, 127.72, 125.85, 125.23, 124.02, 121.71, 119.61, 114.66, 94.72. HRMS (ESI) calcd for [C<sub>19</sub>H<sub>13</sub>NO<sub>2</sub> + H]<sup>+</sup> 288.1025, found 288.10357.

**4.1.5.2 (E)-2-(3-chlorophenyl)-4H-benzo[h]chromen-4-one oxime (11b).** Pale white solid, yield: 81%; <sup>1</sup>H NMR (400 MHz, DMSO-*d*<sub>6</sub>) δ 10.60 (s, 1H), 8.54 – 8.35 (m, 1H), 8.00 (s, 1H), 7.93 – 7.87 (m, 3H), 7.61 – 7.58 (m, 1H), 7.57 (d, *J* = 6.2 Hz, 4H), 7.55 – 7.53 (m, 1H). <sup>13</sup>C NMR (101 MHz, DMSO-*d*<sub>6</sub>) δ 168.29, 161.77, 151.56, 135.34, 134.34, 131.54, 131.40, 130.44, 128.42, 128.11, 126.72, 126.35, 125.78, 125.73, 123.94, 123.30, 120.77, 110.07, 101.64. HRMS (ESI) calcd for [C<sub>19</sub>H<sub>12</sub>ClNO<sub>2</sub> + H]<sup>+</sup> 322.0635, found 322.06382.

**4.1.5.3 (E)-2-(4-chlorophenyl)-4H-benzo[h]chromen-4-one oxime (11c).** Pale white solid, yield: 74%; <sup>1</sup>H NMR (400 MHz, DMSO-*d*<sub>6</sub>) δ 10.64 (s, 1H), 8.46 (s, 1H), 8.01 (d, *J* = 7.2 Hz, 2H), 7.93 (d, *J* = 9.0 Hz, 2H), 7.75 – 7.57 (m, 5H), 7.53 (s, 1H). <sup>13</sup>C NMR (101 MHz, DMSO-*d*<sub>6</sub>) δ 168.14, 161.90, 151.50, 135.31, 135.23, 129.67, 128.87, 128.42, 128.20, 128.08, 126.35, 125.70, 123.91, 123.26, 120.77, 110.08, 101.50. HRMS (ESI) calcd for [C<sub>19</sub>H<sub>12</sub>ClNO<sub>2</sub> + H]<sup>+</sup> 322.0635, found 322.06414.

## 4.2 CYP1 enzyme inhibition assay

EROD (7-ethoxyresorufin O-deethylase) has been used for determining the inhibitory activity of these synthesized compounds against recombinant human CYP1 enzymes, according to our previously reported procedure[14, 16]. The recombinant human CYP1 enzymes (CYP1B1, CYP1A1, and CYP1A2, each equipped with P450 reductase (Supersomes)), were purchased from BD Genetest (Corning). 7-Ethoxyresorufin (7-ER) was available from Sigma-Aldrich. Nicotinamide-adenine dinucleotide phosphate (NADP<sup>+</sup>), D-glucose-6-phosphate (G-6-P) and glucose-6-phosphate dehydrogenase (G-6-PD) were obtained from the company of Biosharp. Generally, a mixture with a final volume of 200 µl containing different concentrations (the final concentrations were 0.5, 1, 5, 10, 50, 100, 500 and 1000 nM, respectively) of tested compounds (except positive and negative control wells), an enzyme source (20 fmol CYP1B1, 10 fmol CYP1A1 or 60 fmol CYP1A2), substrate (7-ER, 150 nM), a NADPH regeneration system containing NADP<sup>+</sup> (1.3 mM), G-6-P (3.3 mM), G-6-PD (0.5 U/ml) and MgCl<sub>2</sub> (3.3 mM) was incubated in a black 96-well flat-bottomed microplate at 37 °C for varied time durations (incubation time for CYP1B1, CYP1A1, and CYP1A2 was 35, 15 and 50 min, respectively). Then, the reaction was quenched by addition of 100 µl of pre-cooled methanol to all wells. Lastly, the fluorescence intensity was measured by FlexStation 3 apparatus with excitation and

emission filters at 544 and 590 nm, respectively. Three replicates were used for each concentration. The  $IC_{50}$  value for each compound was calculated with the GraphPad Prism Software (Version 5.0) using the non-linear regression formula, log (inhibitor) vs. normalized response-variable slope.

### 4.3 Molecular docking procedure

The X-ray structure coordinates of ANF bound with CYP1B1 (PDB ID 3PM0) or CYP1A2 (PDB ID 2HI4) were downloaded from RCSB protein data bank (<http://www.rcsb.org/>). The modelling experiment described in this study was performed by using the docking program of MOE 2008 as our previously described[14]. All water molecules in the crystal structure of CYP1B1 were removed prior to docking. However, in light of the importance of water molecules in formation of water-mediated hydrogen bond, water molecules in the crystal structure of CYP1A2 were retained for docking study.

### 4.4 CoMFA and CoMSIA analysis

In this work, predictive 3D-QSAR models CoMFA and CoMSIA were performed using SYBYL-X 2.0 software from Tripos, Inc. The  $IC_{50}$  values were transformed into  $pIC_{50}$  ( $-\log_{10}(IC_{50} \cdot 10^{-9})$ ) values and used as the dependent variable in CoMFA and CoMSIA analysis. The 3D structures of these CYP1B1 inhibitors were constructed with SYBYL/Sketch module and energy minimization were implemented using the Tripos force field with convergence criterion of 0.005 kcal/(Å<sup>3</sup>·mol) and a maximum of 1000 iterations and Gasteiger-Hückel charges. Based on the variety of activity and structure diversity, all the forty-two ANF derivatives were divided into training set and test set. As one of the most active molecule, compound **9j** was chosen as a main template and the other molecules were aligned to it. In CoMFA study, all aligned molecules were located at the center of grid box with a 3D regularly spaced grid of 2.0 Å using an  $sp^3$  hybridized carbon atom as a probe with +1.0 charge to calculate steric and electrostatic fields. The default cut-off energy value was set at 30 kcal/mol for both steric and electrostatic fields. Partial least squares (PLS) analysis was used to linearly correlate CoMFA fields with the activity values. Cross-validation was performed using the leave-one-out(LOO) method. CoMSIA similarity index descriptors were calculated using a similar lattice box as in CoMFA. For CoMSIA descriptors, five similarity index fields (steric, electrostatic, hydrophobic, hydrogen bond donor, and hydrogen bond acceptor) were calculated using an  $sp^3$  carbon with a charge, hydrophobic interaction, and hydrogen-bond donor and acceptor properties of +1.0 was used as a probe at every grid point to measure the five above-mentioned fields. The default value of 0.3 was used as attenuation factor. All of the contours represented the default 80% and 20% level contributions for favored and disfavored areas, respectively.

### Conflicts of interest

The authors declare no conflicts of interest.



## Acknowledgements

The research reported in this publication was supported by the Interdisciplinary Program of Shanghai Jiao Tong University (project number: ZH2018QNB15), the Fundamental Research Funds for the Central University (No. ZH2018QNB15), the Shanghai Natural Science Fund (No. 16ZR1418100), as well as the Shanghai Science and Technology Innovation Program (No. 15431900700). We also want to express our gratitude to associate professor Xiaoyan Pan and professor Jie Zhang in the Xi'an Jiaotong University for providing SYBYL-X 2.0 software.

## References

- [1] G. I. Murray, M. C. Taylor, M. C. McFadyen, J. A. McKay, W. F. Greenlee, M. D. Burke, W. T. Melvin, Tumor-specific expression of cytochrome P450 CYP1B1, *Cancer Res.*, 57 (1997) 3026-3031.
- [2] M. Nakajima, M. Iwanari, T. Yokoi, Effects of histone deacetylation and DNA methylation on the constitutive and TCDD-inducible expressions of the human CYP1 family in MCF-7 and HeLa cells, *Toxicol. Lett.*, 144 (2003) 247-256.
- [3] M. W. Haque, S. P. Pattanayak, Taxifolin Inhibits 7,12-Dimethylbenz(a)anthracene-induced Breast Carcinogenesis by Regulating AhR/CYP1A1 Signaling Pathway, *Pharmacogn. Mag.*, 13 (2018) S749-S755.
- [4] J. C. Rowlands, L. He, R. Hakkak, M. J. Ronis, T. M. Badger, Soy and whey proteins downregulate DMBA-induced liver and mammary gland CYP1 expression in female rats, *J. Nutr.*, 131 (2001) 3281-3287.
- [5] E. H. Han, Y. P. Hwang, T. C. Jeong, S. S. Lee, J. G. Shin, H. G. Jeong, Eugenol inhibit 7,12-dimethylbenz[a]anthracene-induced genotoxicity in MCF-7 cells: Bifunctional effects on CYP1 and NAD(P)H: quinone oxidoreductase, *FEBS Lett.*, 581 (2007) 749-756.
- [6] J. Dong, Q. Zhang, Q. Cui, G. Huang, X. Pan, S. Li, Flavonoids and Naphthoflavonoids: Wider Roles in the Modulation of Cytochrome P450 Family 1 Enzymes, *ChemMedChem*, 11 (2016) 2102-2118.
- [7] M. C. McFadyen, H. L. McLeod, F. C. Jackson, W. T. Melvin, J. Doehmer, G. I. Murray, Cytochrome P450 CYP1B1 protein expression: a novel mechanism of anticancer drug resistance, *Biochem Pharmacol.*, 62 (2001) 207-212.
- [8] B. Rochat, J. M. Morsman, G. I. Murray, W. D. Figg, H. L. McLeod, Human CYP1B1 and anticancer agent metabolism: mechanism for tumor-specific drug inactivation?, *J. Pharmacol. Exp. Ther.*, 296 (2001) 537-541.
- [9] R. Dutour, F. Cortes-Benitez, J. Roy, D. Poirier, Structure-Based Design and Synthesis of New Estrane-Pyridine Derivatives as Cytochrome P450 (CYP) 1B1 Inhibitors, *ACS Med. Chem. Lett.*, 8 (2017) 1159-1164.
- [10] R. Dutour, D. Poirier, Inhibitors of cytochrome P450 (CYP) 1B1, *Eur. J. Med. Chem.*, 135 (2017) 296-306.
- [11] T. Shimada, H. Yamazaki, M. Foroozesh, N. E. Hopkins, W. L. Alworth, F. P. Guengerich, Selectivity of polycyclic inhibitors for human cytochrome P450s 1A1, 1A2,

and 1B1, Chem. Res. Toxicol., 11 (1998) 1048-1056.

[12] A. Datta, N. Bhasin, H. Kim, M. Ranjan, B. Rider, Z.Y. Abd Elmageed, D. Mondal, K.C. Agrawal, A. B. Abdel-Mageed, Selective targeting of FAK-Pyk2 axis by alpha-naphthoflavone abrogates doxorubicin resistance in breast cancer cells, Cancer Lett., 362 (2015) 25-35.

[13] M. Kubo, K. Yamamoto, T. Itoh, Design and synthesis of selective CYP1B1 inhibitor via dearomatization of  $\alpha$ -naphthoflavone, Bioorg. Med. Chem., 27 (2019) 285-304.

[14] J. Cui, Q. Meng, X. Zhang, Q. Cui, W. Zhou, S. Li, Design and synthesis of new  $\alpha$ -naphthoflavones as cytochrome P450 (CYP) 1B1 inhibitors to overcome docetaxel-resistance associated with CYP1B1 overexpression, J. Med. Chem., 58 (2015) 3534-3547.

[15] J. Y. Dong, Z. T. Wang, Q. Q. Meng, Q. J. Zhang, G. Huang, J. H. Cui, S. S. Li, Development of 2-arylbenzo[h]quinolone analogs as selective CYP1B1 inhibitors, RSC Adv., 8 (2018) 15009-15020.

[16] J. Dong, J. Cui, Y. Wu, S. Li, Q. Meng, Q. Zhang, Z. Wang, G. Huang, Development of benzochalcone derivatives as selective CYP1B1 inhibitors and anticancer agents, MedChemComm, 10 (2019) 1606-1614.

[17] H. Nakazumi, T. Ueyama, Kitao, Teijiro, Synthesis and antibacterial activity of 2-phenyl-4*H*-benzo [*b*] thiopyran-4-ones (Thioflavones) and related compounds, J. Heterocycl. Chem., 21 (1984) 193-196.

[18] D. Vyawahare, M. Ghodke, A. P. Nikalje, Green synthesis and pharmacological screening of novel 1, 5-benzothiazepines as CNS agents, Int. J. Pharm. Pharm. Sci., 2 (2010) 27-29.

[19] A. Wang, U. Savas, C. D. Stout, E. F. Johnson, Structural characterization of the complex between alpha-naphthoflavone and human cytochrome P450 1B1, J. Biol. Chem., 286 (2011) 5736-5743.

[20] S. Sansen, J. K. Yano, R. L. Reynald, G. A. Schoch, K. J. Griffin, C. D. Stout, E. F. Johnson, Adaptations for the oxidation of polycyclic aromatic hydrocarbons exhibited by the structure of human P450 1A2, J. Biol. Chem., 282 (2007) 14348-14355.

[21] A. A. Walsh, G. D. Szklarz, E. E. Scott, Human cytochrome P450 1A1 structure and utility in understanding drug and xenobiotic metabolism, J. Biol. Chem., 288 (2013) 12932-12943.

## Highlights

- Discovery of two potent CYP1B1 inhibitors with high selectivity;
- Provided comprehensive structure-activity relationships of  $\alpha$ -naphthoflavone derivatives as CYP1 inhibitors;
- Expanding SAR with a range of phenyl ring replacements would lay a foundation for development of ANF-based water-soluble CYP1B1 inhibitors.



**Conflicts of interest**

The authors declare no conflicts of interest.